Institute for Space Nuclear Power Studies
Department of Chemical and Nuclear Engineering
The University of New Mexico
Albuquerque, New Mexico 87131

Cs-Ba TACITRON: II. IGNITION CHARACTERISTICS DURING BREAKDOWN AND CURRENT MODULATION MODES

MOHAMED EL-GENK, BEN WERNSMAN, AND CHRIS MURRAY

DISTRIBUTION STATEMENT A
Approved for public release
Distribution Unlimited

FINAL REPORT NO. UNM-ISNPS 2-1992

Subcontract No. S-247-002-001, UES Services Inc., Dayton, Ohio

Performance Period March 1, 1991 - February 12, 1992

PLEASE RETURN TO:

BMD TECHNICAL INFORMATION CENTER
BALLISTIC MISSILE DEFENSE ORGANIZATION
7100 DEFENSE PENTAGON
WASHINGTON D.C. 20301-7100

19980309 179

March 1992

U 4462

Accession Number: 4462

Publication Date: Mar 01, 1991

Title: Cs-Ba Tacitron: II. Ignition Characteristics During Breakdown and Current Modulation Modes

Personal Author: El-Genk, M.; Wernsman, B.; Murray, C.

Corporate Author Or Publisher: Institute for Space Nuclear Power Studies, U. of NM, Albuquerque, NM 8
Report Number: UNM-ISNPS 2-1992

Descriptors, Keywords: Cs-Ba Tacitron Ignition Modulation Mode

Pages: 00060

Cataloged Date: Apr 21, 1993

Contract Number: S-247-002-001,

Document Type: HC

Number of Copies In Library: 000001

Record ID: 26719

Institute for Space Nuclear Power Studies
Department of Chemical and Nuclear Engineering
The University of New Mexico
Albuquerque, New Mexico 87131

Cs-Ba TACITRON: II. IGNITION CHARACTERISTICS DURING BREAKDOWN AND CURRENT MODULATION MODES

MOHAMED EL-GENK, BEN WERNSMAN, AND CHRIS MURRAY

FINAL REPORT NO. UNM-ISNPS 2-1992

Subcontract No. S-247-002-001, UES Services Inc., Dayton, Ohio

Performance Period March 1, 1991 - February 12, 1992

March 1992

TABLE OF CONTENTS

Page

ABSTRACT iii

LIST OF FIGURES iv

NOMENCLATURE vi

1. INTRODUCTION 1

2. OBJECTIVES 3

3. DEVICE DESCRIPTION 3

4. EXPERIMENTAL PROCEDURE 4

5. METHODOLOGY 5

6. RESULTS AND DISCUSSION 9
   6.1 Ignition in the Breakdown Mode 10
   6.2 Ignition in the Modulation Mode 16
   6.3 Ignition Conditions for Stable Current Modulation 34

7. SUMMARY AND CONCLUSION 39

ACKNOWLEDGMENTS 40

REFERENCES 41

Cs-Ba TACITRON: II. IGNITION CHARACTERISTICS DURING BREAKDOWN AND CURRENT MODULATION MODES

ABSTRACT

Experiments are performed to determine the effects of the emitter temperature, Cs pressure, Ba pressure, and grid and collector voltages on the ignition of the Cs-Ba tacitron in the breakdown and current modulation modes. The values of off-time required for ignition in the breakdown mode are compared with those in the modulation mode for both stable and unstable current modulation conditions. Results show that in both modes of operation, the off-time required for ignition is strongly dependent on the Cs pressure in the gap and the applied positive grid potential but less dependent on the emitter temperature and the Ba pressure. Increasing the Cs pressure and/or the grid potential causes the off-time for ignition to decrease. It is determined that the net adsorption/desorption of Cs atoms onto the cold electrode surfaces during the off-time is negligible. Reducing the grid potential not only increases the off-time, hence decreasing modulation frequency of the device, but also can under certain conditions, cause current modulation to become unstable. Results show that the ignition duty cycle threshold for stable modulation is about 40-60 %, regardless of the values of the applied positive grid potential. This threshold is weakly dependent on the Cs pressure, Ba pressure and the applied modulation frequency to the grid. However, increasing the grid potential for ignition beyond that corresponding to the duty cycle threshold causes the off-time required for ignition to decrease and the duty cycle of the device to increase.

LIST OF FIGURES

Page

Figure 1. A Typical Timing Diagram of the Cs-Ba Tacitron During Stable Current Modulation 2

Figure 2. Measured Signals Illustrating the Conditions of the Cs-Ba Tacitron During the Breakdown Mode of Operation 11

Figure 3. Effect of Cs Pressure and Collector Voltage on the Grid Potential for Ignition in the Breakdown Mode 12

Figure 4. Effect of Emitter Temperature on the Grid Potential for Ignition in the Breakdown Mode at T_{Ba} = 500 °C 14

Figure 5. Effect of Emitter Temperature on the Grid Potential for Ignition in the Breakdown Mode at T_{Ba} = 530 °C 15

Figure 6. Effect of Cesium Reservoir Temperature on the Off-time for Ignition in the Modulation Mode of Operation at T_E = 1200 °C, T_{Ba} = 500 °C, and f_g = 2 kHz 17

Figure 7. Effect of Cesium Reservoir Temperature on the Off-time for Ignition in the Modulation Mode of Operation at T_E = 1250 °C, T_{Ba} = 500 °C, and f_g = 2 kHz 18

Figure 8. Effect of Cesium Reservoir Temperature on the Off-time for Ignition in the Modulation Mode of Operation at T_E = 1300 °C, T_{Ba} = 500 °C, and f_g = 2 kHz 19

Figure 9. Effect of Cesium Reservoir Temperature on the Off-time for Ignition in the Modulation Mode of Operation at T_E = 1250 °C, T_{Ba} = 530 °C, and f_g = 3 kHz 21

Figure 10. Effect of Emitter Temperature on the Off-time for Ignition in the Modulation Mode of Operation at T_{Cs} = 155 °C, T_{Ba} = 500 °C, and f_g = 3 kHz 22

Figure 11. Effect of Emitter Temperature on the Off-time for Ignition in the Modulation Mode of Operation at T_{Cs} = 155 °C, T_{Ba} = 530 °C, and f_g = 3 kHz 23

Figure 12. Effect of Cs Adsorption During Stable Current Modulation on Calculated Pad for Ignition Compared to the Measured Pad from Breakdown Mode Data for T_E = 1200 °C and T_{Ba} = 500 °C 24

Figure 13. Effect of Cs Adsorption During Stable Current Modulation on Calculated Pad for Ignition Compared to the Measured Pad from Breakdown Mode Data for T_E = 1300 °C and T_{Ba} = 500 °C 26

Figure 14. Effect of Cs Adsorption During Stable Current Modulation on Calculated Pad for Ignition Compared to the Measured Pad from Breakdown Mode Data for T_E = 1200 °C and T_{Ba} = 530 °C 27

Page

Figure 15. Effect of Cs Adsorption During Stable Current Modulation on Calculated Pad for Ignition Compared to the Measured Pad from Breakdown Mode Data for T_E = 1300 °C and T_{Ba} = 530 °C.....28

Figure 16. Comparison of the Effect of V_{g+} on the Off-time Required for Ignition in the Breakdown and Modulation Modes.....30

Figure 17. Typical Operation Characteristics of the Cs-Ba Tacitron for Stable Modulation at a Positive Grid Potential of 30 V and T_{Cs} = 150 °C.....31

Figure 18. Typical Operation Characteristics of the Cs-Ba Tacitron for Unstable Modulation at a Positive Grid Potential of 20 V and T_{Cs} = 150 °C.....32

Figure 19. Effect of Cesium Reservoir Temperature on the Off-time for Ignition in the Off-time Current Modulation Mode of Operation Compared to the Calculated Value of at f_g = 2 kHz.....33

Figure 20. Effect of Ignition Grid Potential and Cesium Reservoir Temperature on the Duty Cycle of the Cs-Ba Tacitron for a f_m = 2 kHz and T_E = 1200 °C.....35

Figure 21. Effect of Ignition Grid Potential and Cesium Reservoir Temperature on the Duty Cycle of the Cs-Ba Tacitron for a f_m = 2 kHz and T_E = 1250 °C.....36

Figure 22. Effect of Ignition Grid Potential and Cesium Reservoir Temperature on the Duty Cycle of the Cs-Ba Tacitron for a f_m = 2 kHz and T_E = 1300 °C.....37

Figure 23. Effect of Ignition Grid Potential and Cesium Reservoir Temperature on the Duty Cycle of the Cs-Ba Tacitron for a f_m = 3 kHz and T_E = 1250 °C.....38

NOMENCLATURE

τ_m	: Modulation period of tacitron (s)
τ_{off}	: Off-time of discharge (s)
τ_{rise}	: Rise-time of discharge (s)
τ_{on}	: On-time of discharge (s)
τ_{fall}	: Fall-time of discharge (s)
τ_{ad}	: Anode delay-time (s)
τ_{g-}	: Pulse width of negative grid voltage (s)
τ_{g-max}	: Pulse width of maximum negative grid voltage (s)
τ_g	: Applied grid period (s)
V_{ce}	: Applied voltage between collector and emitter (V)
V_d	: Voltage drop between collector and emitter (V)
V_{g+}	: Applied positive grid voltage (V)
V_{g-}	: Applied negative grid voltage (V)
I_c	: Discharge current to collector (A)
I_g	: Grid current (A)
P_{Cs}	: Cs reservoir vapor pressure (torr)
P_{Ba}	: Ba reservoir vapor pressure (torr)
P_a	: Cs vapor pressure in the gap (torr)
$\overline{v_a}$	: Thermal velocity of Cs atoms in the gap (m/s)
k	: Boltzmann's constant (J/K)
σ_a	: Cs surface atom density (m^2)
A_g	: Sum of collector and grid surface areas (m^2)
T_E	: Emitter temperature (K)
T_C	: Collector temperature (K)
T_g	: Grid temperature (K)
T_{Cs}	: Cesium reservoir temperature (K)
T_{Ba}	: Barium reservoir temperature (K)
T_a	: Arithmetic average of the emitter and collector temperatures (K)
T_f	: Basis flange temperature (K)
n_a	: Cs atom density in the gap ($atoms/m^3$)
n_a'	: Cs atom density in the gap required for ignition ($atoms/m^3$)
n_{ae}	: Heavy particle density in the gap at the time of extinguishing ($particles/m^3$)
Γ_a	: Cs atom flux entering the gap ($atoms/m^2s$)
Γ_a'	: Cs atom flux leaving the gap ($atoms/m^2s$)
V_{dr}	: Sum of the emitter-grid gap and grid hole volumes (m^3)
S	: Area through which Cs enters the gap from the reservoir (m^2)
d	: Distance between emitter and grid (m)
N_a	: Number of Cs atoms in the gap
M_a	: Mass of Cs atom (kg)
fm	: Modulation frequency of tacitron, $1/\tau_m$ (Hz)
fg	: Applied modulation frequency to grid, $1/\tau_g$ (Hz)
η_d	: Duty cycle, $(\tau_g-\tau_{off})/\tau_g$ (%)

1. INTRODUCTION

The Cs-Ba tacitron is a thermionic converter filled with a low pressure mixture of cesium and barium (< 25 mtorr) with a third electrode (grid). The Cs vapor neutralizes the space charge in the interelectrode gap and the Ba vapor increases the emission current. The grid, which is placed between the emitter and collector, is used to ignite "turn-on" and extinguish "turn-off" the device by applying a positive and a negative potential on the grid, respectively. Because the tacitron is inherently radiation and thermal hard and could be operated at a modulation frequency up to 20 kHz, it is suitable for inverting DC signals to AC signals in many space power applications.[1-3] However, the device's conduction losses and modulation frequency will determine which applications it is best suited for. Recently, stable modulation of a Cs-Ba tacitron at a switching frequency up to 8 kHz and conduction losses as low as 4 volts have been demonstrated.[1] A typical timing diagram showing the I-V characteristics of both the collector and grid of the Cs-Ba tacitron during current modulation mode of operation is shown in Fig. 1. As can be seen, the modulation frequency, f_m, of the Cs-Ba tacitron is defined as the reciprocal of the modulation period, τ_m, which is approximately equal to the sum of the off-time, τ_{off}, and on-time, τ_{on}, of the device.

As delineated in Fig. 1, the off-time is approximately equal to the duration of the negative grid pulse plus the anode delay time, τ_{ad}. Therefore, in order to increase the modulation frequency of the device, the anode delay time needs to be made as short as possible. The off-time of the device affects the anode delay time as well as the positive grid potential required to ignite the discharge.[3,4] The anode delay time, is the time lapse between the application of a positive potential to the grid and the actual ignition of the device (see Fig. 1). Recently, Murray, El-Genk and Kaibyshev [2-4] have shown that during the modulation mode of operation the discharge in the Cs-Ba tacitron initially occurs between the emitter and the grid. However, further studies are needed to understand and quantify the effects of the different design and operation parameters (such as the emitter temperature, Ba and Cs vapor pressures, grid and collector voltages, width of

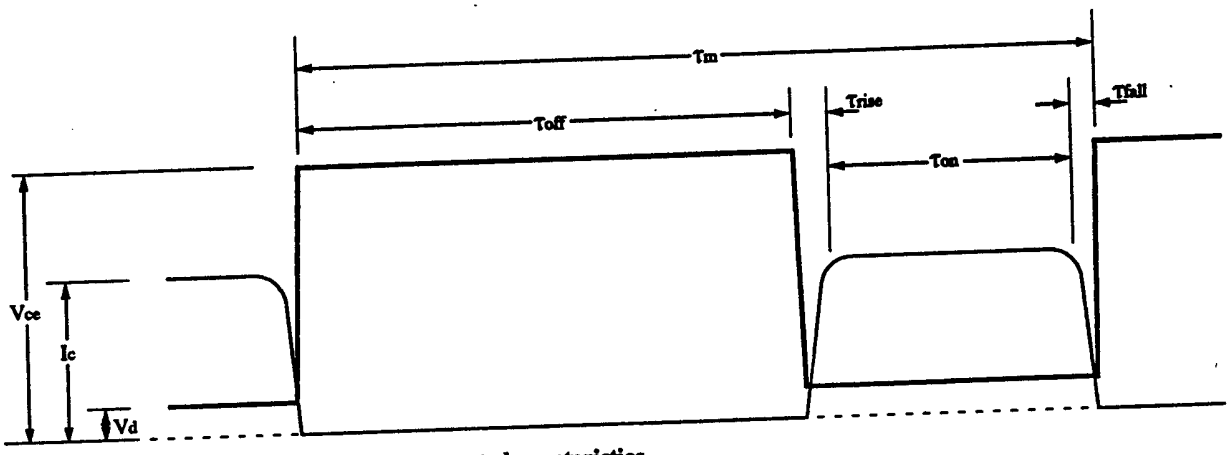

a) Typical collector voltage and current characteristics

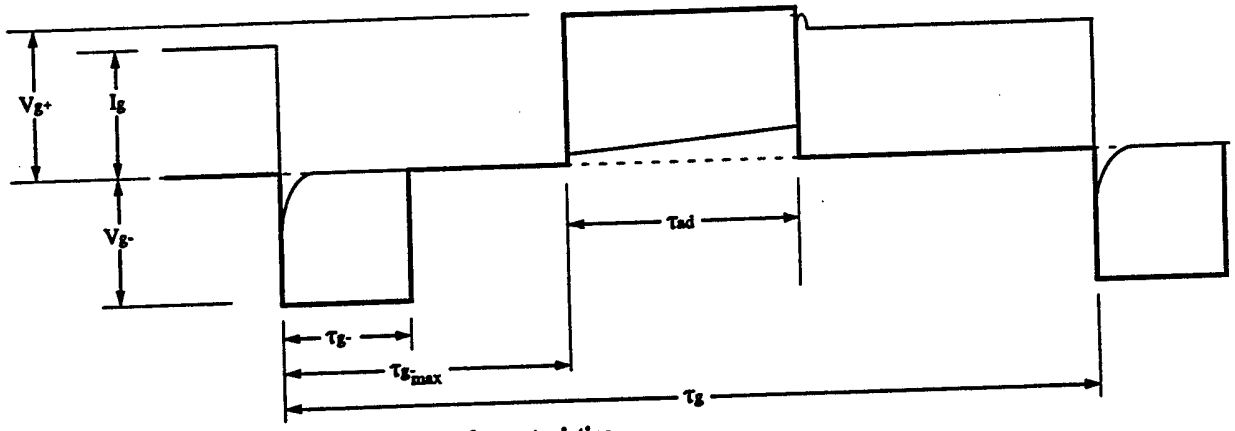

b) Typical grid voltage and current characteristics

Voltage
Current
Stable Modulation Occurs when τm=τg

Figure 1. A Typical Timing Diagram of the Cs-Ba Tacitron During Stable Current Modulation

emitter-grid gap and the net adsorption on the cold surfaces) on the off-time required for ignition of the Cs-Ba tacitron during both the breakdown and modulation modes of operation.

2. OBJECTIVES

The objectives of this work are to perform experiments to determine the effects of the operating parameters including the emitter temperature, Cs pressure, Ba pressure, grid voltage and collector voltage on the ignition of the Cs-Ba tacitron in the breakdown and current modulation modes. Also, the effect of the net adsorption of Cs atoms onto the cold surfaces during stable current modulation is studied. To determine the applicability of the ignition data in the breakdown mode to the modulation mode of operation,[4] the off-time for the former is compared with those of the latter, for stable and unstable current modulation conditions. The experimental data is also used to determine the off-time required for successful ignition, and the effects of the aforementioned operation parameters on the ignition duty cycle threshold for stable modulation.

3. DEVICE DESCRIPTION

The Cs-Ba tacitron device used in the experiments consists of one diode section and two triode sections, each has a separate grid. All three sections have a common emitter but separate collectors.[1] The off-time measurements during both the breakdown and modulation modes are made on the bottom triode section. The assembled device is mounted on top of a stainless-steel basis flange. The flange is heated to prevent condensation of the Cs and Ba vapor on the walls. The Cs and Ba vapors diffuse through the internal cavities in the flange before entering the interelectrode gap of the tacitron. The Cs reservoir is equipped with a long narrow orifice to minimize diffusion of Ba vapor and contamination of the Cs reservoir.

The emitter, grid and collector are all constructed of molybdenum. In the bottom triode section, the spacing between the emitter and grid is 1 mm, and the spacing between the emitter and collector is 4.25 mm. The grid is 1 mm thick and has 0.8 mm holes and physical transparency ~ 34 %. The Cs and Ba vapor pressures in the gap are independently controlled by external electric

heaters on their respective reservoirs. The electric heater for the emitter is a 2 mm diameter tungsten rod. The rod is surrounded by a tantalum tube, which returns the current from the heater to the power supply and prevents a magnetic field from developing due to the high heater current. The temperature of the emitter is monitored by three W-Re thermocouples, which are located in the emitter at elevations which correspond to the positions of the respective collector sections. The temperatures of the grid and the collector sections as well as those of the Cs and Ba reservoirs are measured using type-K thermocouples. For a more extensive description of the device, refer to El-Genk et al.[1] and Murray, El-Genk and Kaibyshev.[3]

4. EXPERIMENTAL PROCEDURE

In the present experiments, measurements are always made after the Cs and Ba pressures and the temperatures of the device have reached steady-state. When the device is first turned on, a waiting period of one to two hours is required for the device to reach steady-state. Subsequently, a change of one of the operating parameters (for example, emitter temperature, Cs pressure, or Ba pressure) would require a much shorter waiting period, on the order of five to ten minutes, for the device to reach steady-state. In the experiments, the Cs reservoir temperature is varied from 120 °C (1.76 mtorr) to 165 °C (17.1 mtorr), while the Ba reservoir temperature is kept at either 500 °C (0.02 mtorr) or 530 °C (0.07 mtorr), and the emitter temperature is kept at either 1200 °C or 1300 °C. The ignition potential to the grid is varied from 5 V to 30 V. In the breakdown experiments, the emitter temperature, Ba pressure, Cs pressure and the ignition potential to the grid are maintained constant, while a half-sinusoidal voltage pulse to the collector is applied to determine the collector voltage when ignition occurs (see Fig. 2). In these experiments, the amplitude of the voltage pulse to the collector is kept constant at 170 V. By independently varying the Cs pressure, Ba pressure and the emitter temperature, the collector voltage for ignition in the breakdown mode is determined as a function of the applied positive potential to the grid, V_{g+}.

In the experiments involving the modulation mode of operation, the collector voltage is kept constant at 150 V. At the selected values of the Cs pressure, Ba pressure and emitter temperature,

the off-times for stable and unstable modulation of the tacitron are measured as functions of the applied grid voltage to cause ignition.

5. METHODOLOGY

Following ignition of the Cs-Ba tacitron, the Cs atom density in the interelectrode gap decreases. This rarefaction of Cs atoms in the Cs-Ba tacitron comes about because of the high degree of plasma ionization and high electron temperature which results in the removal of ions from the interelectrode gap.[2,3] For subsequent ignition to occur, the concentration of Cs atoms in the gap would have to recover to some definite value; otherwise, the device will fail to ignite. The recovery of the Cs atoms in the gap by diffusion from the surrounding region depends on the density of heavy components in the gap at the time of extinguishing the previous discharge, n_{ae}, the Cs reservoir pressure (i.e. Cs reservoir temperature), and the length of the off-time. The amount of Cs atoms in the gap will affect the anode delay time and/or the magnitude of the grid potential needed for successful ignition.

Because the anode delay time is an important portion of the off-time, reducing the anode delay time would subsequently reduce the off-time for ignition. There are six parameters which affect the anode delay time, τ_{ad}, of the Cs-Ba tacitron: (a) the magnitude of the positive grid potential, V_{g+}, (b) the time between extinguishing and the application of the positive grid potential, $\tau_{g\text{-}max}$, (c) the duration of on-time, τ_{on}, (d) the value of collector current, I_c, during the discharge, (e) the cesium vapor pressure, and (f) the forward conduction voltage drop, V_d. In order to increase the repetition frequency of the device, it is important to quantify the effects of these parameters on the off-time required for successful ignition of the device. In this paper, we investigated the effects of Cs pressure, Ba pressure, emitter temperature, and the applied grid potential, V_{g+}, on the off-time for ignition. The effects of the remaining parameters ($\tau_{g\text{-}max}$, τ_{on}, I_c, and V_d) are currently being investigated.

The grid potential for successful ignition is measured during both breakdown and stable current modulation conditions. In the experiments investigating ignition in the breakdown mode,

the waiting period to reach steady-state (five minutes) is more than sufficient to establish equilibrium conditions in the interelectrode gap, a priori. When these conditions are established, the flux of Cs atoms entering the gap from the Cs reservoir equals that leaving the gap to the surroundings and the Cs atoms in the gap are at thermal equilibrium with the electrodes. The equilibrium density of Cs atoms in the gap is then given by:

$$n_a = \frac{133P_a}{kT_a} = n_{Cs}\sqrt{\frac{T_{Cs}}{T_a}}\ , \tag{1}$$

where n_{Cs}, the cesium atom density at the reservoir, is given by

$$n_{Cs} = \frac{133P_{Cs}}{kT_{Cs}}\ . \tag{2}$$

In Eq. (1), T_a is the arithmetic mean temperature of the emitter and collector, and T_{Cs} is the Cs reservoir temperature. The Cs pressure in the gap, P_a, can be expressed as:

$$P_a = P_{Cs}\sqrt{\frac{T_a}{T_{Cs}}}\ . \tag{3}$$

In Eqs. (2) and (3), the Cs pressure in the gap, P_{Cs}, can be expressed as:[5]

$$P_{Cs} = \frac{2.45x10^8}{\sqrt{T_{Cs}}}\exp\left[\frac{-8910}{T_{Cs}}\right]\ . \tag{4}$$

Also, the flux of Cs atoms entering the gap from the surrounding is given by:

$$\Gamma_a = \frac{1}{4}n_a\overline{v_a} = \frac{1}{4}n_{Cs}\sqrt{\frac{T_{Cs}}{T_a}}\sqrt{\frac{8kT_a}{\pi M_a}} = \frac{1}{4}n_{Cs}\sqrt{\frac{8kT_{Cs}}{\pi M_a}}\ . \tag{5}$$

In the experiments, the mean Cs atom temperature in the surrounding gap region, T_a, is ~ 1200 K. For a Cs vapor pressure of 10^{-2} torr, n_a in the gap is approximately $8x10^{14}$ atoms/cm^3 (Eqs. (1) and (2)) and the corresponding atom flux is $8.7x10^{17}$ atoms/cm^{2}s (Eq. (5)). Since the flux of Cs atoms entering the gap is driven by the temperature of the cesium reservoir (Eq. (5)), it does not change whether the device is on or off.[4] Conversely, because during current discharge the ion velocity is larger than the atom velocity, the gas density in the interelectrode gap drops due to ion leakage from the gap to the surrounding region.[4] After the discharge is extinguished, the Cs atom density in the gap begins to recover with time by diffusion of Cs atoms from the surrounding region. Results show that for a certain applied grid potential, in order to ignite the device, the Cs atom density in the gap has to reach a definite value, otherwise ignition will not occur. Also, the off time, τ_{off}, required for the Cs atom density in the gap to reach the definite value required for ignition, n_a', may be expressed as:[3]

$$\tau_{off} = \frac{\Delta N_a}{(\Gamma_a - \Gamma_a')S}, \qquad (6)$$

where ΔN_a is the increase in the amount of Cs atoms in the gap during τ_{off}, which is given by:

$$\Delta N_a = (n_a' - n_{ae})V_{dr} + \Delta\sigma_a A_g . \qquad (7)$$

For Eq. (7), V_{dr} is the volume of the gap, S is the area through which Cs atoms enter the gap from the surrounding region, n_{ae} is the density of Cs atoms in the gap immediately after extinguishing, and A_g is the sum of the grid and collector surface areas where Cs atoms can be adsorbed. The values for V_{dr}, S and A_g for the bottom triode section are 1.5 cm^3, 0.27 cm^2 and ~ 19 cm^2, respectively. $\Delta\sigma_a$ is the change in the Cs surface atom density on the grid and collector surfaces and is a function of the net adsorption/desorption of Cs atoms onto these surfaces during the off-

time. If it assumed that the surface density at the operating temperature of the grid and collector coincide with a monolayer coating of cesium ($2x10^{14}$ atoms/cm^2), then $\Delta\sigma_a$ can be given by

$$\Delta\sigma_a \sim 2x10^{14}\left[\frac{(n_a' - n_{ae})}{n_a}\right] \text{ atoms /cm}^2 \quad . \tag{8}$$

The mean flux of heavy components out of the gap during the discharge is given by:

$$\Gamma_a' = \frac{1}{4}\overline{v_a}\frac{(n_a' + n_{ae})}{2} \sim \frac{1}{4}\overline{v_a}\, n_a' \quad . \tag{9}$$

Therefore, substituting Eqs. (7) through (9) into Eq. (6) gives:

$$\tau_{off} = (n_a' - n_{ae})\left\{\frac{V_{dr} + \frac{2x10^{14}}{n_a}A_g}{\frac{S\ \overline{v_a}}{4}\left(n_{Cs}\sqrt{\frac{T_{Cs}}{T_a}} - n_a'\right)}\right\} \quad . \tag{10}$$

The first term in the numerator is the net change in the amount of Cs atoms in the gap during the off-time, and the second term accounts for the net adsorption/desorption of Cs atoms into/from the surface of the grid and collector during the off-time. From Eq. (10), the density required for ignition during the current modulation mode of operation, n_a', can be expressed as

$$n_a' = \frac{S\, n_{Cs}\tau_{off}\,\overline{v_a}\sqrt{\frac{T_{Cs}}{T_a}} + 4n_{ae}\left(V_{dr} + \frac{2x10^{14}}{n_a}A_g\right)}{S\tau_{off}\,\overline{v_a} + 4V_{dr} + \frac{8x10^{14}}{n_a}A_g} \quad . \tag{11}$$

If the net adsorption of Cs atoms onto the surfaces during the off-time is negligible, then $\Delta\sigma_a$ could be set equal to zero, and Eqs. (10) and (11) are reduced respectively to:

$$\tau_{off} = \frac{(n_a' - n_{ae})V_{dr}}{\frac{S\ \overline{v_a}}{4}\left(n_{Cs}\sqrt{\frac{T_{Cs}}{T_a}} - n_a'\right)}, \qquad (12)$$

and,

$$n_a' = \frac{S\, n_{Cs}\tau_{off}\,\overline{v_a}\sqrt{\frac{T_{Cs}}{T_a}} + 4n_{ae}V_{dr}}{S\tau_{off}\,\overline{v_a} + 4V_{dr}}. \qquad (13)$$

Equations (10) and (12) give the off-time required for successful ignition at a certain Cs reservoir temperature and applied grid potential with and without the effects of Cs adsorption, respectively. Equations (11) and (13) give the required Cs density in the gap for successful ignition as a function of the measured operating conditions (P_{Cs} and T_a) and the off-time, with and without the effect of Cs adsorption onto the cold electrode surfaces, respectively. To ascertain the effect of the Cs adsorption on the off-time during stable current modulation, the calculated value of n_a' is compared with the values determined from the measured Cs pressure in the gap during the breakdown mode of operation of the device. In addition, the effects of the emitter temperature, Ba vapor pressure and Cs reservoir temperature on τ_{off}, n_a' and the positive grid potential required for ignition are investigated experimentally. The results are presented and discussed in the next section.

6. RESULTS AND DISCUSSION

Experimental measurements are made of the collector voltage, V_{ce}, for ignition in the breakdown mode as a function of the following operation parameters: (a) applied positive potential to the grid, V_{g+}, (b) Cs reservoir temperature, T_{Cs}, (c) Ba reservoir temperature, T_{Ba}, and (d) emitter temperature, T_E. This data is used to measure the Cs atom density required for ignition to occur at a given V_{g+} and calculate the off-time, τ_{off}, required to reach this density for a given set of operating conditions. To determine the role of the Cs adsorption/desorption on the off-time for ignition during stable current modulation, the calculated value of n_a', from either Eq. (11) or (13),

for a given set of operating parameters, is compared to the calculated values based on the measured Cs pressure. To determine the effect of the operation mode on τ_{off}, the calculated values for ignition in the breakdown mode are compared with those measured during the stable current modulation mode of operation. In addition, the effects of Cs reservoir temperature, Ba vapor pressure, emitter temperature and operating modulation frequency to the grid on τ_{off} and the device's duty cycle for stable and unstable modulation are determined.

6.1 Ignition in the Breakdown Mode

Figure 2 presents a typical response of the Cs-Ba tacitron operating in the breakdown mode; the operating conditions are shown at the bottom of the graph. As shown in Fig. 2, ignition of the tacitron occurs approximately 7 ms after the application of the breakdown pulse to the collector, at which time the collector voltage drops from 160 V to 10 V and the collector current rises simultaneously from 0 A to 60 A. At the point of ignition the grid potential, V_g, also drops from its pre-ignition value of 5.5 V to zero, while the grid current, I_g, increases from approximately 250 mA to 4.0 A. After 9 ms (or approximately 2 ms following ignition) the collector current and voltage and the grid voltage reaches steady values of 30 A, 12 V and -0.5 V, respectively, while the grid current remains unchanged at 4 A.

The measured values of the collector voltage required for ignition in the breakdown mode, at the same operating conditions as in Fig. 2, are plotted in Fig. 3 versus the applied positive grid potential, V_{g+}, for different Cs reservoir temperatures (or Cs pressure). Figure 3 shows that at a given collector voltage, the grid potential required for ignition in the breakdown mode increases as the Cs reservoir temperature (or Cs pressure) decreases. For example, at a collector voltage of 150 V, the grid potential necessary for ignition increases from 5 V to as much as 24 V as the Cs pressure decreases from 16.4 mtorr (T_{Cs} = 164 °C) to 3.8 mtorr (T_{Cs} = 134 °C). Results in Fig. 3 also show that while the grid potential required for ignition is strongly dependent on the Cs pressure in the gap it is almost independent of the collector voltage, V_{ce}.

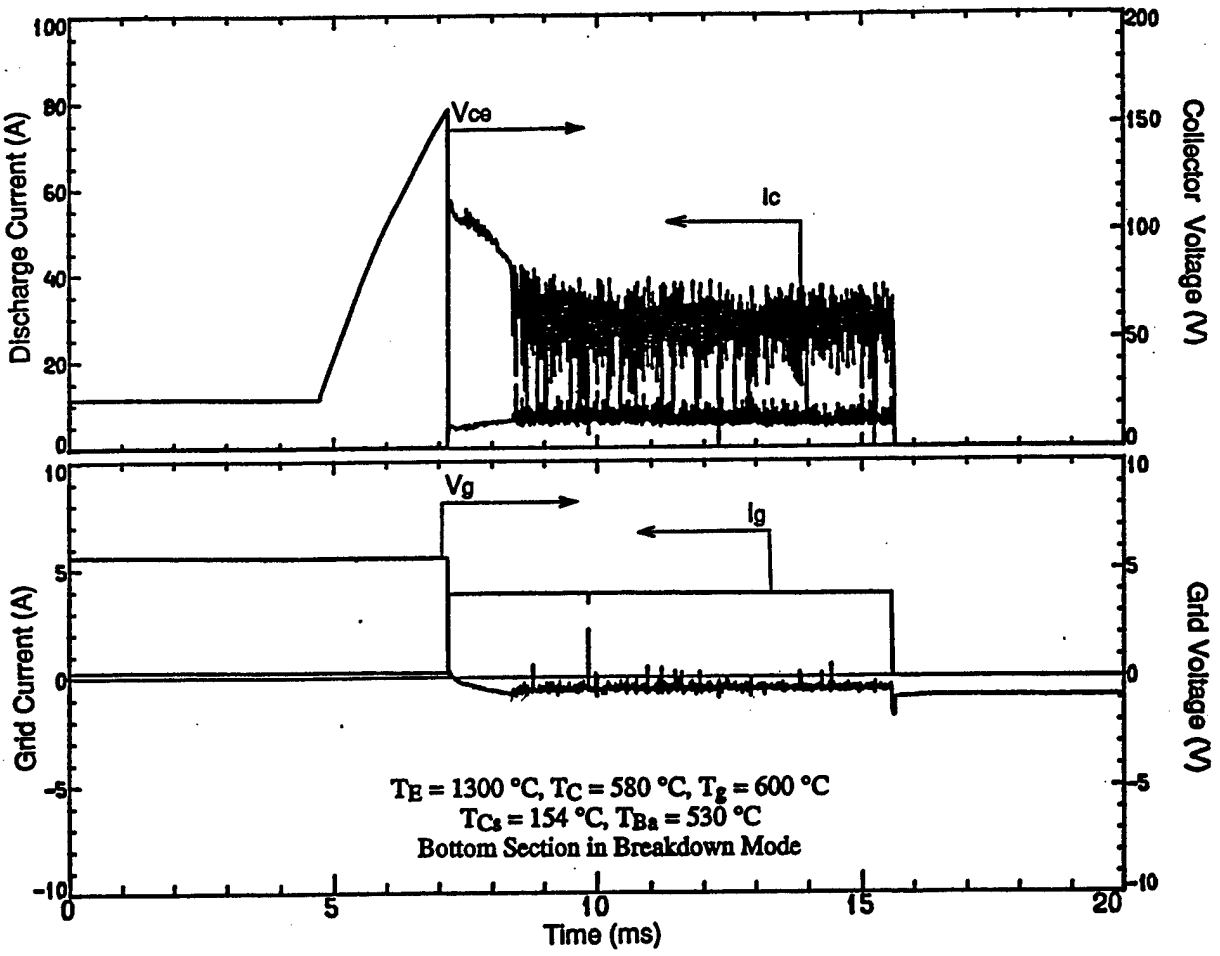

Figure 2. Measured Signals Illustrating the Conditions of the Cs-Ba Tacitron During the Breakdown Mode of Operation

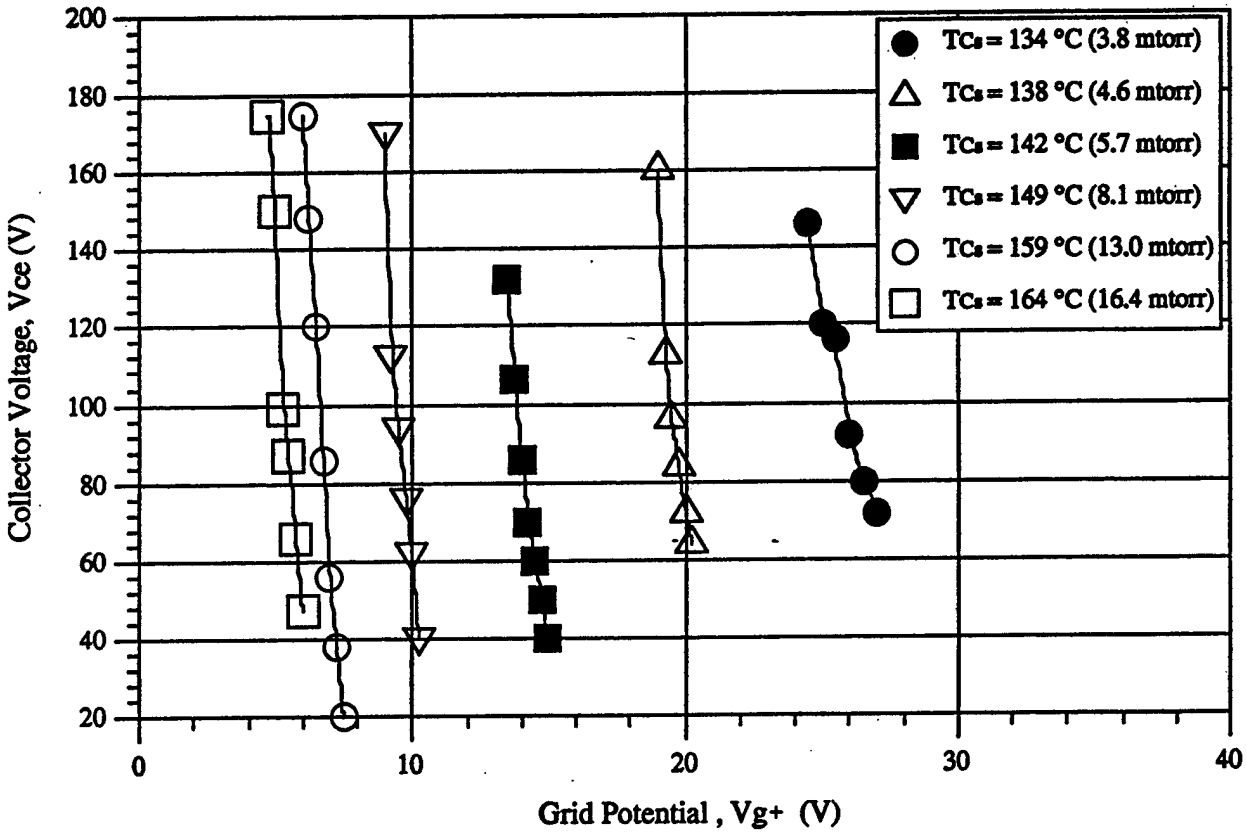

Figure 3. Effect of Cs Pressure and Collector Voltage on the Grid Potential for Ignition in the Breakdown Mode

Additional experiments are performed to measure the effects of changing the Ba pressure and/or the emitter temperature on the grid potential required for ignition in the breakdown mode. The results are presented in Figs. 4 and 5. In these figures the grid voltage for ignition is plotted versus the P_ad parameter, where d is the distance between the emitter and grid (1 mm), and P_a is the Cs pressure in the gap (in torr). The gap between the emitter and grid is used for the P_ad parameter in Figs. 4 and 5, since it has been demonstrated that the discharge initially ignites in the emitter-grid region [4]. Again, these figures demonstrate that the collector voltage insignificantly affects the grid potential for ignition, while the effects of the emitter temperature and Ba pressure are small. Figure 4 shows that at a Ba temperature of 500 °C (P_{Ba} = 0.02 mtorr) and a given P_ad value, increasing the emitter temperature from 1200 °C to 1300 °C reduces the grid potential for ignition. For an example, at a P_ad value of 0.01 mm-torr the grid potential for ignition decreases from 13 V to 11.5 V as the emitter temperature is increased from 1200 °C to 1300 °C. For P_ad values less than 0.01 mm-torr, the difference between the grid voltages required for ignition at these two emitter temperatures increases as P_ad is decreased, while for P_ad values greater than 0.01 mm-torr, this difference in V_{g+} becomes very small. It is worth noting that at P_ad values higher than 0.025 mm-torr, the grid potential for ignition becomes almost independent of P_ad.

Figures 4 and 5 indicate that when the Ba reservoir temperature is increased from 500 °C (P_{Ba} = 0.02 mtorr) to 530 °C (P_{Ba} = 0.07 mtorr) the effect of the emitter temperature on the grid potential for ignition is reversed, such that increasing the emitter temperature from 1200 °C to 1300 °C increases the required grid voltage for ignition. This reversal will be examined in more detail in the next section from the calculated Cs density required for ignition via the measured off-time during stable current modulation. For example, at a P_ad value of 0.01 mm-torr, the grid potential for ignition increases from 13 V to 14 V as the emitter temperature is increased from 1200 °C to 1300 °C. Figure 5 also shows that the effect of emitter temperature on the difference in V_{g+} for ignition at T_E of 1200 °C and 1300 °C is approximately the same for all P_ad values (~ 1 V). A comparison of the data in Figs. 4 and 5 shows that at T_E = 1200 °C the grid potential for ignition is almost independent of T_{Ba}; however, at the higher emitter temperature of 1300 °C, the Ba vapor

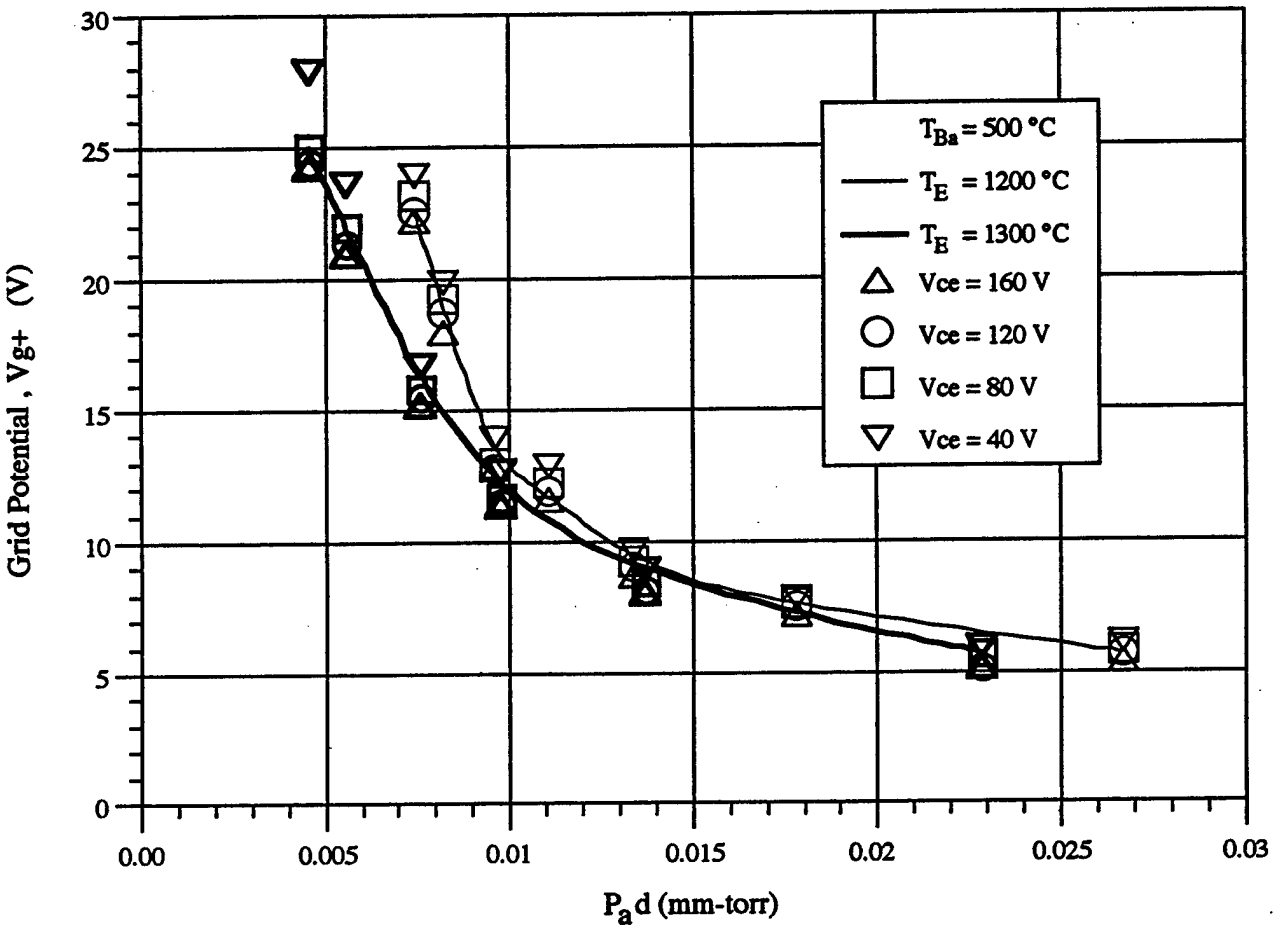

Figure 4. Effect of Emitter Temperature on the Grid Potential for Ignition in the Breakdown Mode at T_{Ba} = 500 °C

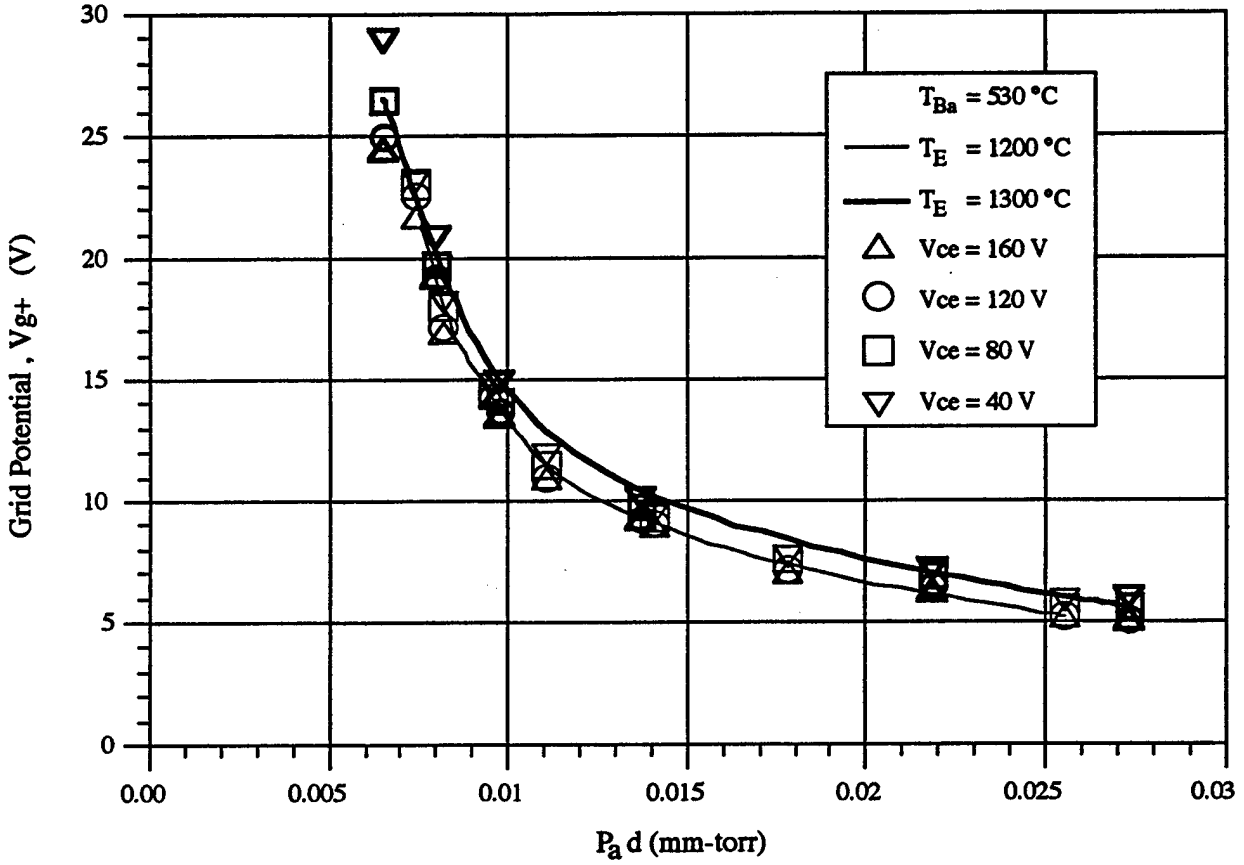

Figure 5. Effect of Emitter Temperature on the Grid Potential for Ignition in the Breakdown Mode at T_{Ba} = 530 °C

pressure affects the grid potential for ignition whereas increasing P_{Ba} increases the grid potential required for ignition. For example, at a $P_a d$ of 0.01 mm-torr and T_E = 1200 °C, the grid potential of 13 V in Fig. 5 is identical to that shown in Fig. 4 at the same emitter temperature but lower P_{Ba} (T_{Ba} = 500 °C). On the other hand at an emitter temperature of 1300 °C, the grid potential increases from 11.5 V to 14 V (~ 40%) as the Ba reservoir temperature increases from 500 °C to 530 °C.

6.2 Ignition in the Modulation Mode

The $P_a d$ values in Figs. 4 and 5 directly correspond to the densities of Cs atoms, n_a', in the gap which are required to successfully ignite the Cs-Ba tacitron in the breakdown mode. To determine the effect of the net Cs adsorption occurring during the off-time of stable current modulation, the value of n_a' calculated from Eq. (11) and (13) are compared to these values corresponding to the Cs pressure for ignition in the breakdown mode from Figs. 4 and 5. To achieve this, the off-time during current modulation is measured, and the results are shown in Figs 6-11, for various emitter temperatures (T_E), Ba pressures (T_{Ba}), Cs pressures (T_{Cs}) and applied modulation frequencies (f_g). As can be seen in Fig. 6, the off-time required for ignition during stable current modulation decreases as the Cs pressure is increased. For example, at V_{g+} = 25 V, τ_{off} decreases from 220 μs to 120 μs as T_{Cs} is increased from 150 °C to 160 °C. Also, as V_{g+} is increased, the off-time decreases and becomes almost independent of V_{g+} beyond 35 V. As an example, for T_{Cs} = 160 °C, τ_{off} increases from 100 μs to 200 μs as V_{g+} is decreases from 30 V to 20 V. For Vg+ less than 20 V (τ_{off} ~ 260 μs), a large jump in the off-time occurs because current modulation becomes unstable; whereas $f_m < f_g$. During unstable current modulation, ignition of the discharge occurs when a positive potential is applied to the grid, but the discharge fails to extinguish intermittently when a negative potential is applied to the grid, resulting in a longer off-time. Based on the results presented in Fig. 6, it is concluded that a necessary condition for the calculation of n_a' at f_g = 2 kHz is that $\tau_{off} \leq 260$ μs.

Similar results of the measured off-time during the current modulation mode as a function of V_{g+} for three different Cs reservoir temperatures, are obtained and presented in Figs. 7 and 8.

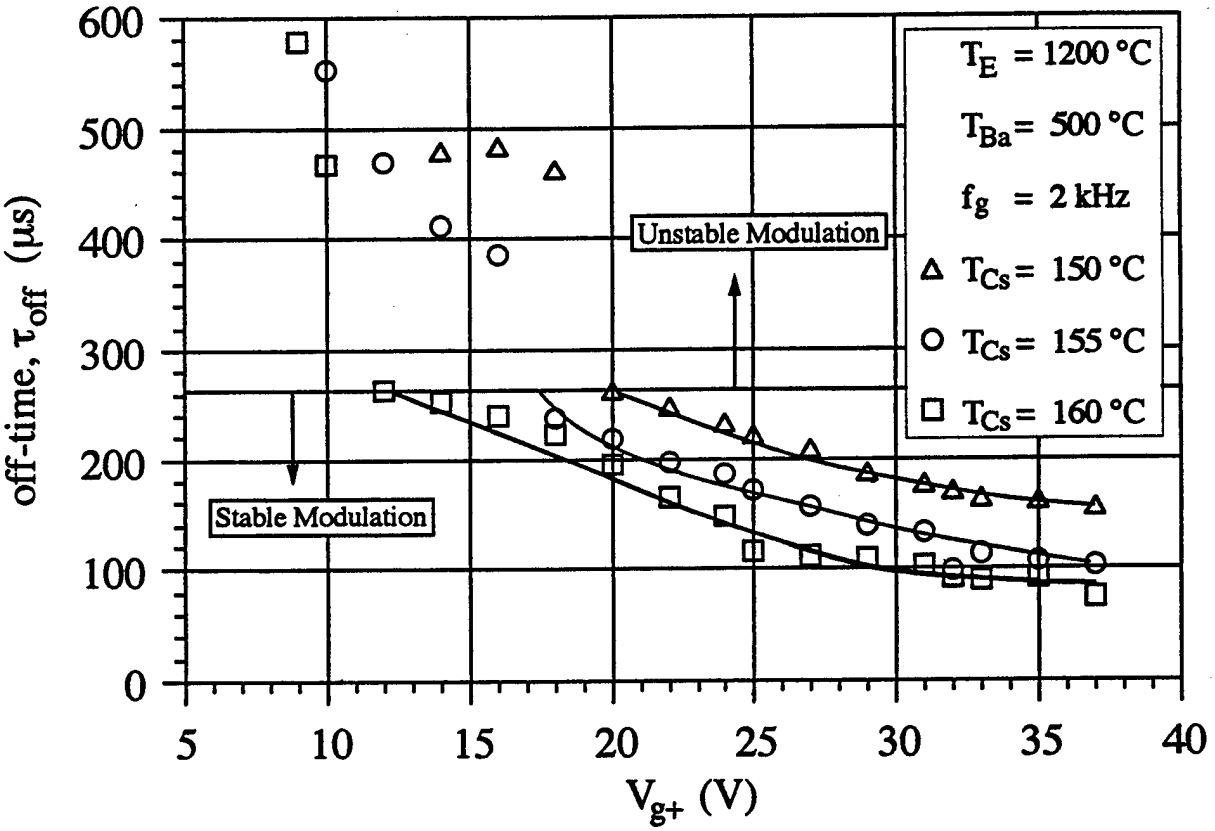

Figure 6. Effect of Cesium Reservoir Temperature on the Off-time for Ignition in the Modulation Mode of Operation at T_E = 1200 °C, T_{Ba} = 500 °C, and f_g = 2 kHz

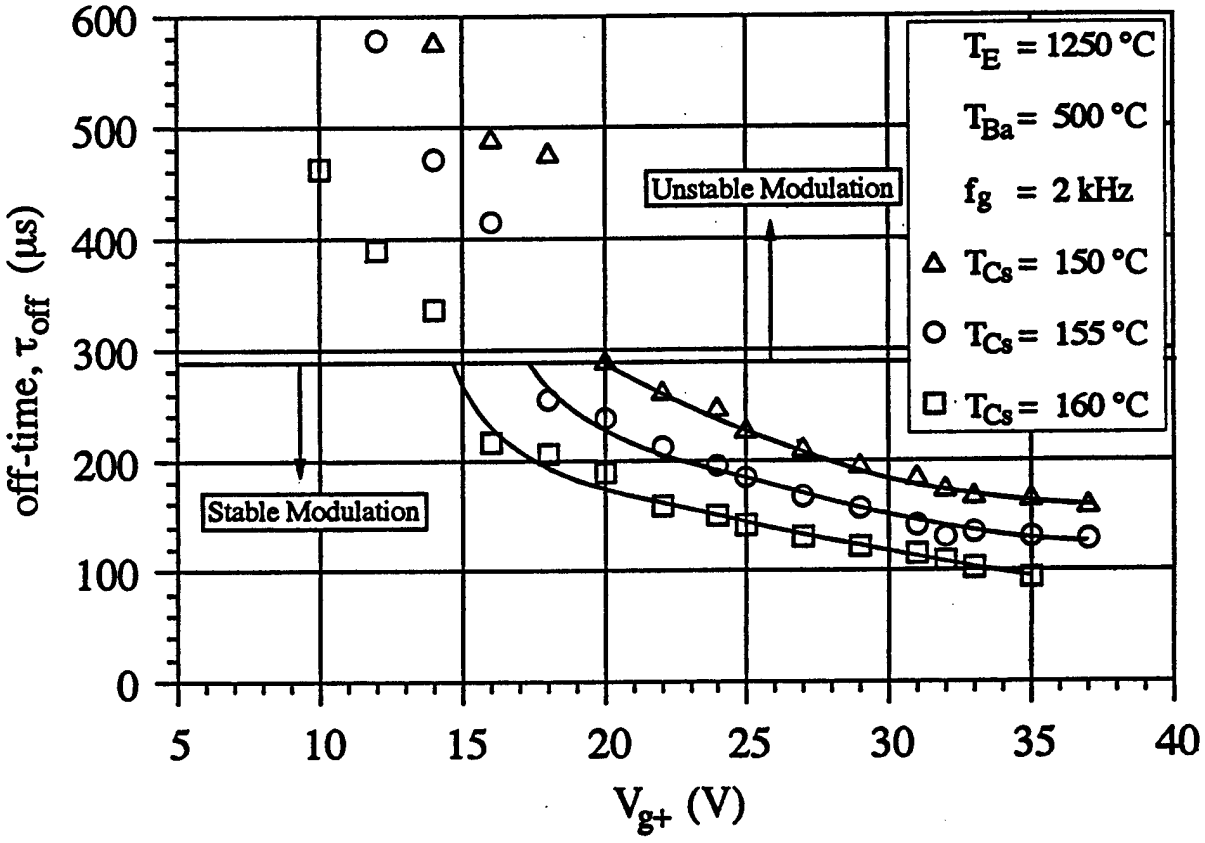

Figure 7. Effect of Cesium Reservoir Temperature on the Off-time for Ignition in the Modulation Mode of Operation at T_E = 1250 °C, T_{Ba} = 500 °C, and f_g = 2 kHz

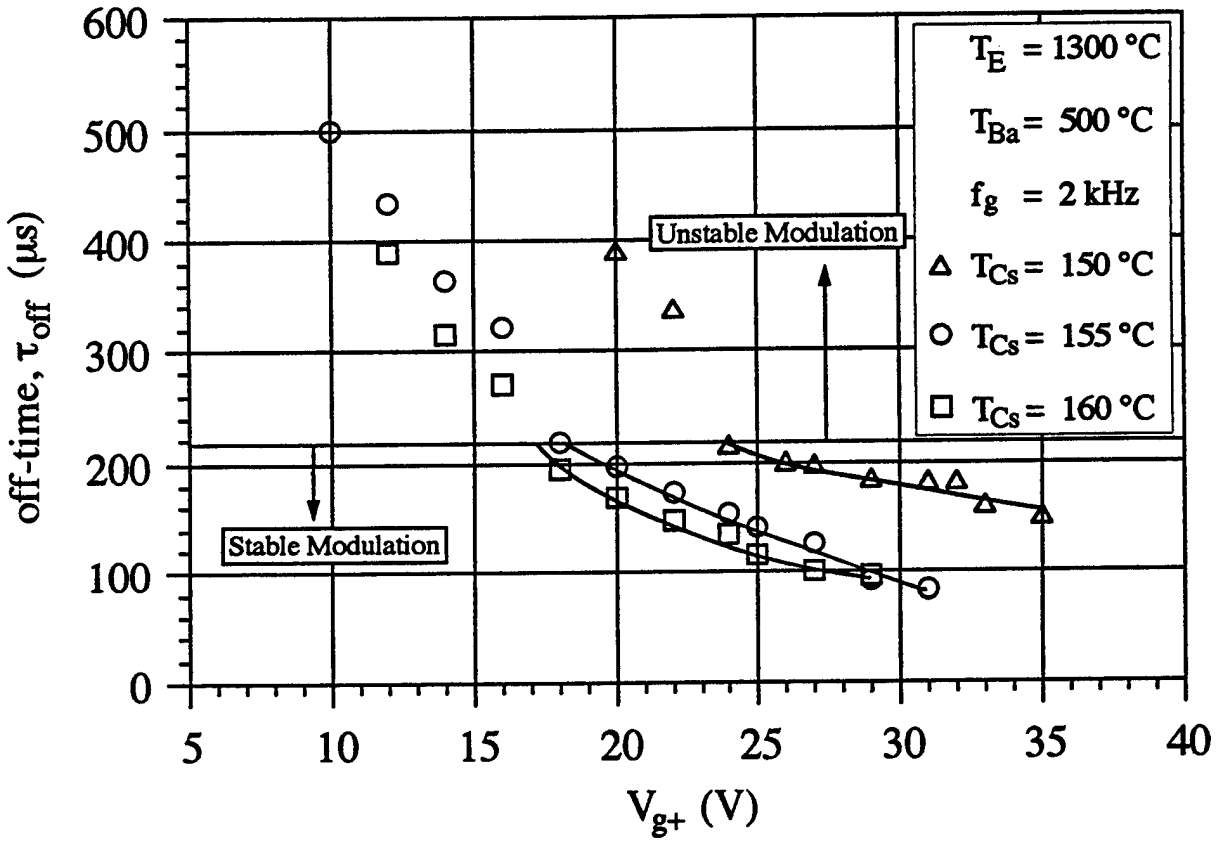

Figure 8. Effect of Cesium Reservoir Temperature on the Off-time for Ignition in the Modulation Mode of Operation at T_E = 1300 °C, T_{Ba} = 500 °C, and f_g = 2 kHz

As Figs. 6-8 show, increasing the emitter temperature slightly increases the values of τ_{off} for stable current modulation. However, the threshold for unstable current modulation decreases from ~ 260 μs at T_E = 1200 °C (Fig. 6) to ~ 210 μs at T_E = 1300 °C (Fig. 8).

Figures 9-11 show the measured off-time as a function of V_{g+} for a modulation frequency of 3 kHz. Figure 9 shows the same dependances of τ_{off} on V_{g+} and Cs pressures as those delineated Fig. 7, except that the valued of τ_{off} at the same V_{g+} is significantly lower. Figure 7 also shows that increasing the grid modulation frequency from 2 kHz to 3 kHz reduces not only the values of τ_{off}, but also its threshold for stable current modulation. Figures 10 and 11 give the measured off-time as a function of V_{g+} for two emitter temperatures (1200 °C and 1300 °C) at T_{Cs} = 155 °C. As can be seen in Figs. 9-11, stable current modulation occurs when $\tau_{off} \leq 200$ μs. These τ_{off} values for stable modulation are used to calculate n_a'. The results in Fig. 10 show that for $V_{g+} > 30$ V, τ_{off} for stable current modulation is independent of the V_{g+} value . At lower V_{g+} values, however, τ_{off} increases as T_E is increased. For an example, at V_{g+} = 25 V, increasing T_E from 1200 °C to 1300 °C increases τ_{off} from 140 μs to 170 μs (~21%).

Figures 12-15 show the calculated and measured P_ad values for ignition in the stable current modulation and the breakdown mode, as a function of V_{g+} for T_{Cs} = 155 °C, f_g = 3 kHz, and for different emitter and Ba reservoir temperatures. The calculated values are obtained from the stable current modulation off-times measurements (see Figs. 6-11). As can be seen in Fig. 12, the calculated values of P_ad for ignition during stable current modulation with a net Cs adsorption term (Eq. (11)) is approximately 0.003 mm-torr, which is independent of V_{g+}, and far from the measured P_ad values for ignition in the breakdown mode. On the other hand, using the formulation without a net Cs adsorption during the off-time (Eq. (13)), the calculated P_ad values lie close to, but are smaller than those from the breakdown mode. Since in this last case, the calculated and measured values are close to each other, it is believed that the effects of Cs adsorption, if any, insignificantly influences the off-time required to restore the Cs density in the gap in order for ignition to occur during stable current modulation.

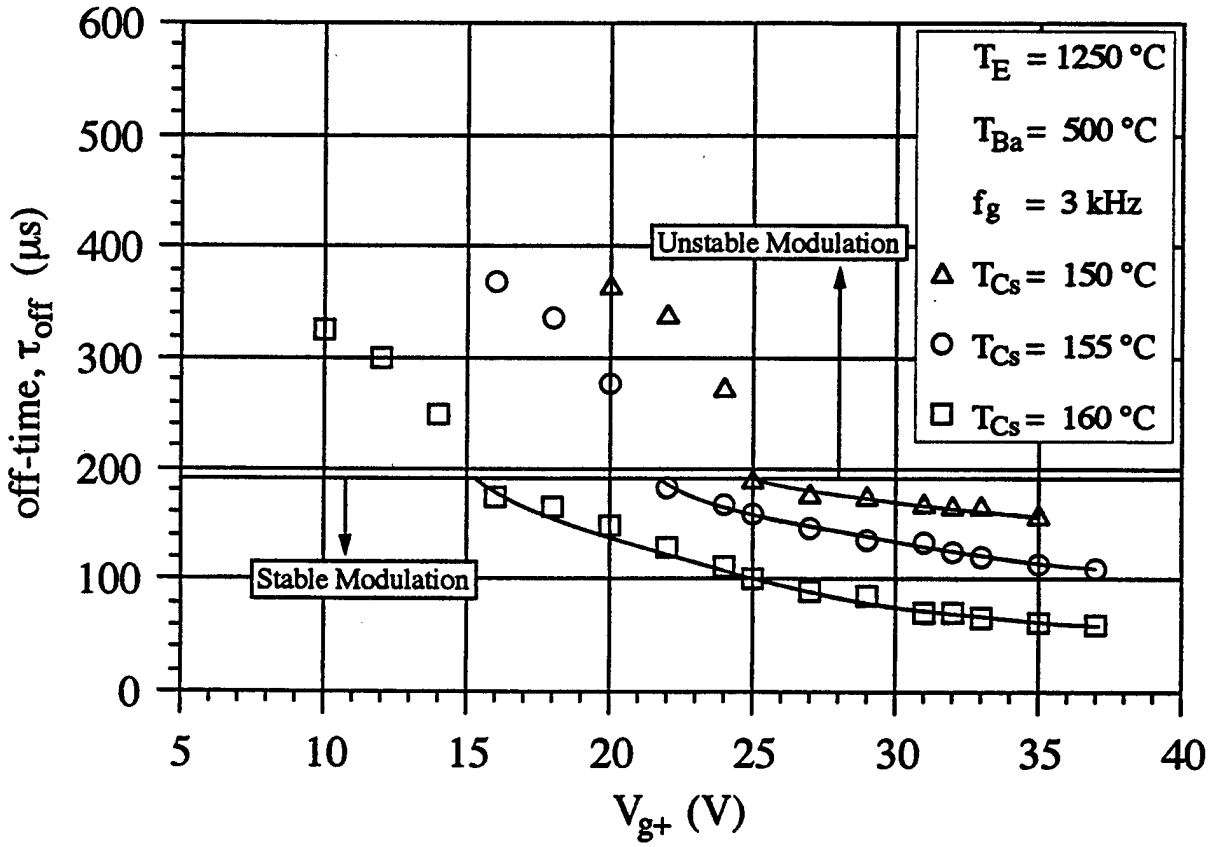

Figure 9. Effect of Cesium Reservoir Temperature on the Off-time for Ignition in the Modulation Mode of Operation at T_E = 1250 °C, T_{Ba} = 530 °C, and f_g = 3 kHz

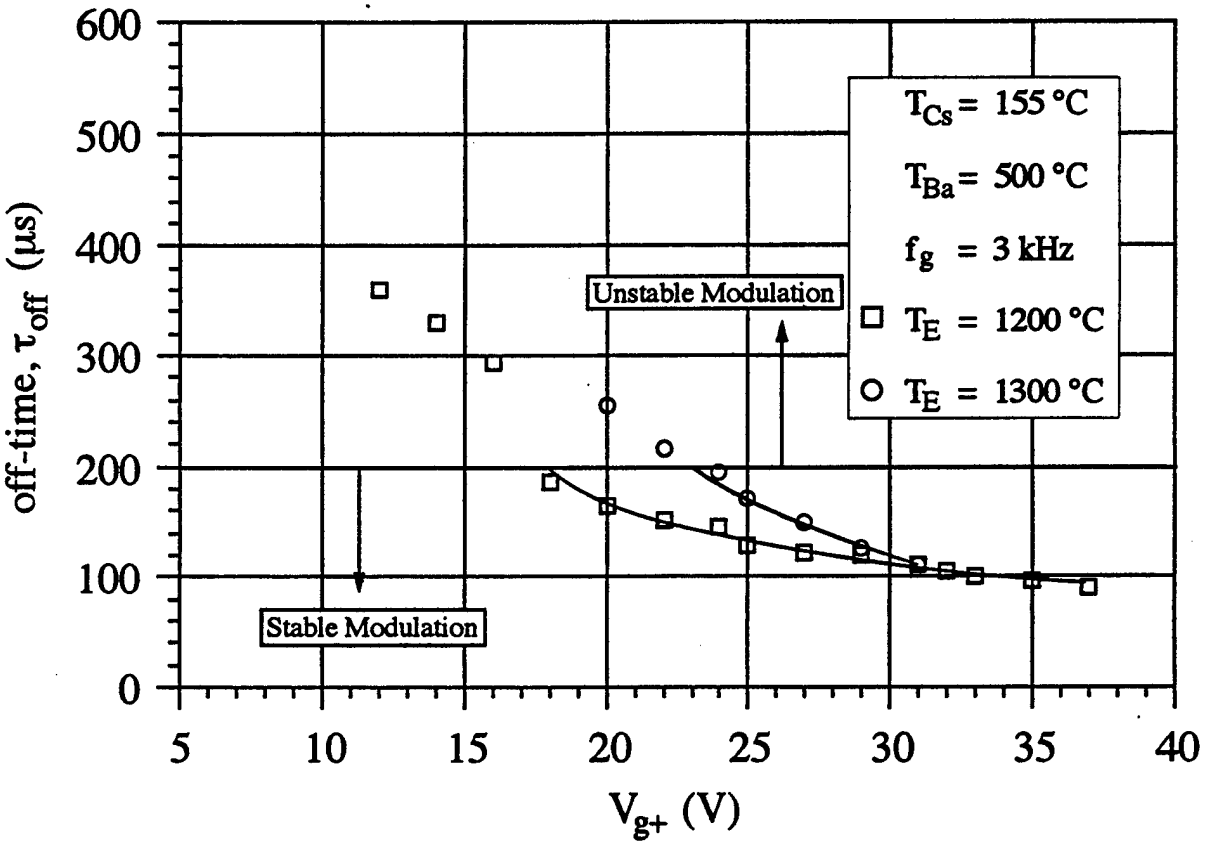

Figure 10. Effect of Emitter Temperature on the Off-time for Ignition in the Modulation Mode of Operation at T_{Cs} = 155 °C, T_{Ba} = 500 °C, and f_g = 3 kHz

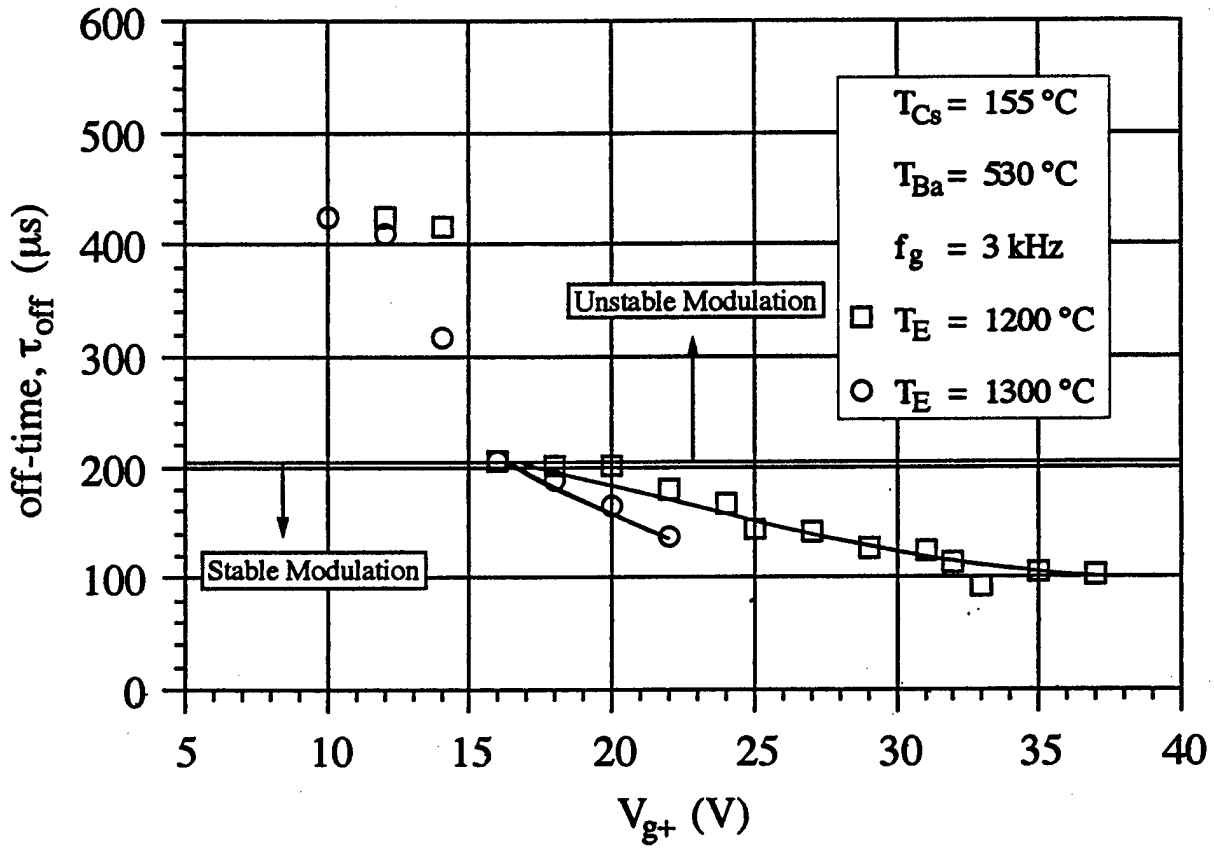

Figure 11. Effect of Emitter Temperature on the Off-time for Ignition in the Modulation Mode of Operation at T_{Cs} = 155 °C, T_{Ba} = 530 °C, and f_g = 3 kHz

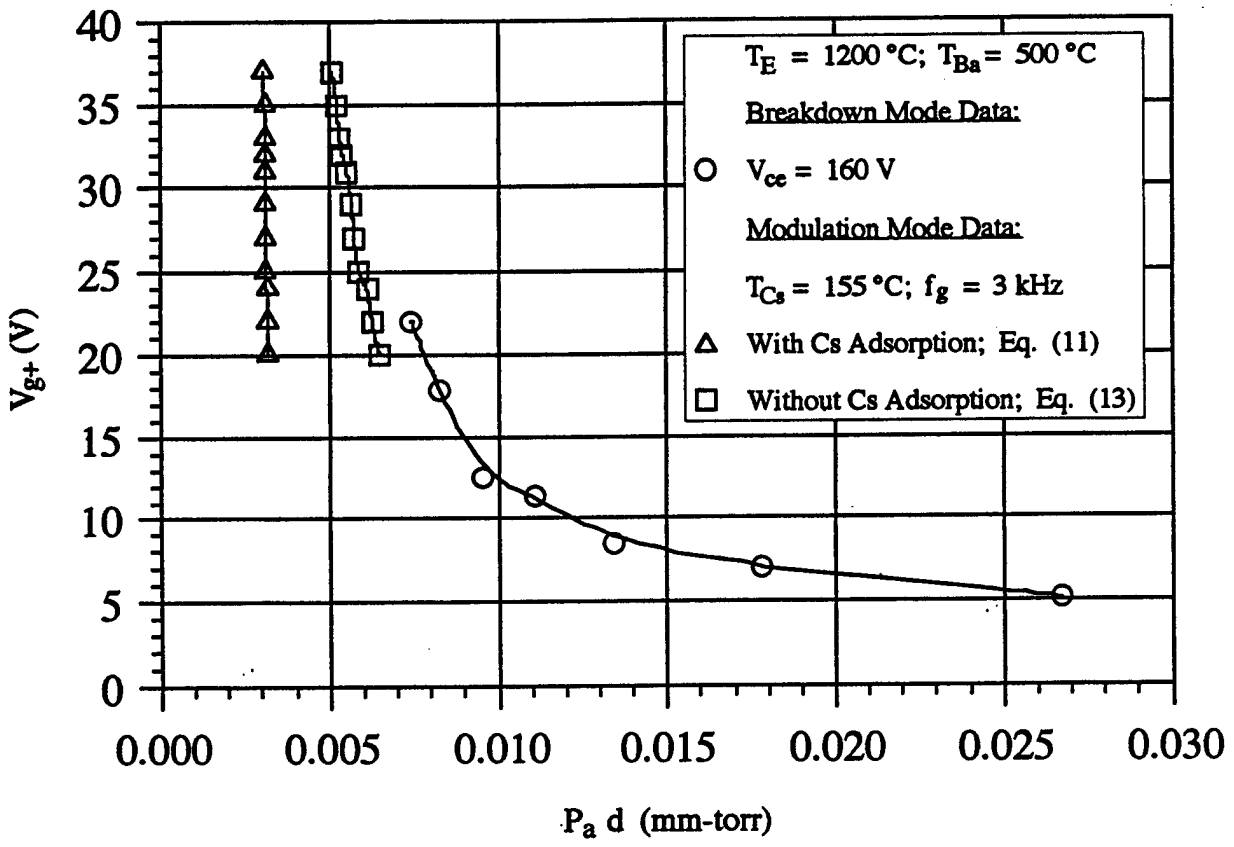

Figure 12. Effect of Cs Adsorption During Stable Current Modulation on Calculated P_ad for Ignition Compared to the Measured P_ad from Breakdown Mode Data for T_E = 1200 °C and T_{Ba} = 500 °C

Similar results are shown in Figs. 13-15. However, as can be seen in Fig. 13, the measured P_ad values for ignition in the breakdown mode lie between the calculated values from Eq. (11) and (13). Since this is the only measured P_ad data that does this and, as previously mentioned, the influence of the emitter temperature is reversed from that observed for T_{Ba} = 530 °C (Fig. 4 and 5), it is concluded that these measured values of P_ad for T_E = 1300 °C and T_{Ba} = 500 °C are not accurate. This inaccuracy could be caused by the fact that the operating parameters (T_{Ba}, T_{Cs} and T_E) in the device had not reached equilibrium when the measurements were taken. Additional measurements of the P_ad for ignition during the breakdown mode of operation are needed to clarify this error.

As previously stated, the P_ad values from Fig. 4 and 5 (excluding the T_E = 1300 °C and T_{Ba} = 500 °C curve) correspond to the densities of Cs atoms, n_a', in the gap, which are required to successfully ignite the discharge in the Cs-Ba tacitron. These densities are used in Eq. (12) (no net Cs adsorption as seen in Figs. 12-15) to calculate the corresponding off-times required for the Cs atoms to recover to their values for ignition. The calculated off-times are plotted versus the applied positive grid potential for ignition in Fig. 16. These off-time values are also compared with those measured for ignition during the modulation mode of operation at T_E = 1300 °C, T_{Ba} = 530 °C and T_{Cs} = 150 °C and a grid modulation frequency of 4 kHz. As shown in Fig. 16, the off-time for ignition in the stable current modulation mode of operation is always lower than that calculated from the breakdown mode. For an applied grid potential greater than 24 V, the measured off-time during stable current modulation are almost the same for both pulse mode modulation times of 3 ms and 13 ms. This indicates that the discharge conditions change very little for pulse mode modulation times greater than 3 ms. This time equals that needed for the plasma in the gap to reach equilibrium during the discharge.[4]

The data in Fig. 16 also demonstrates that in order to reduce the off-time during modulation, and hence increase the modulation frequency of the tacitron, V_{g+} should be increased. A high grid potential forces ignition between the emitter and grid at lower Cs atom concentrations, hence smaller τ_{off}. At a modulation time of 3.0 ms, when the grid potential is increased from 25 V

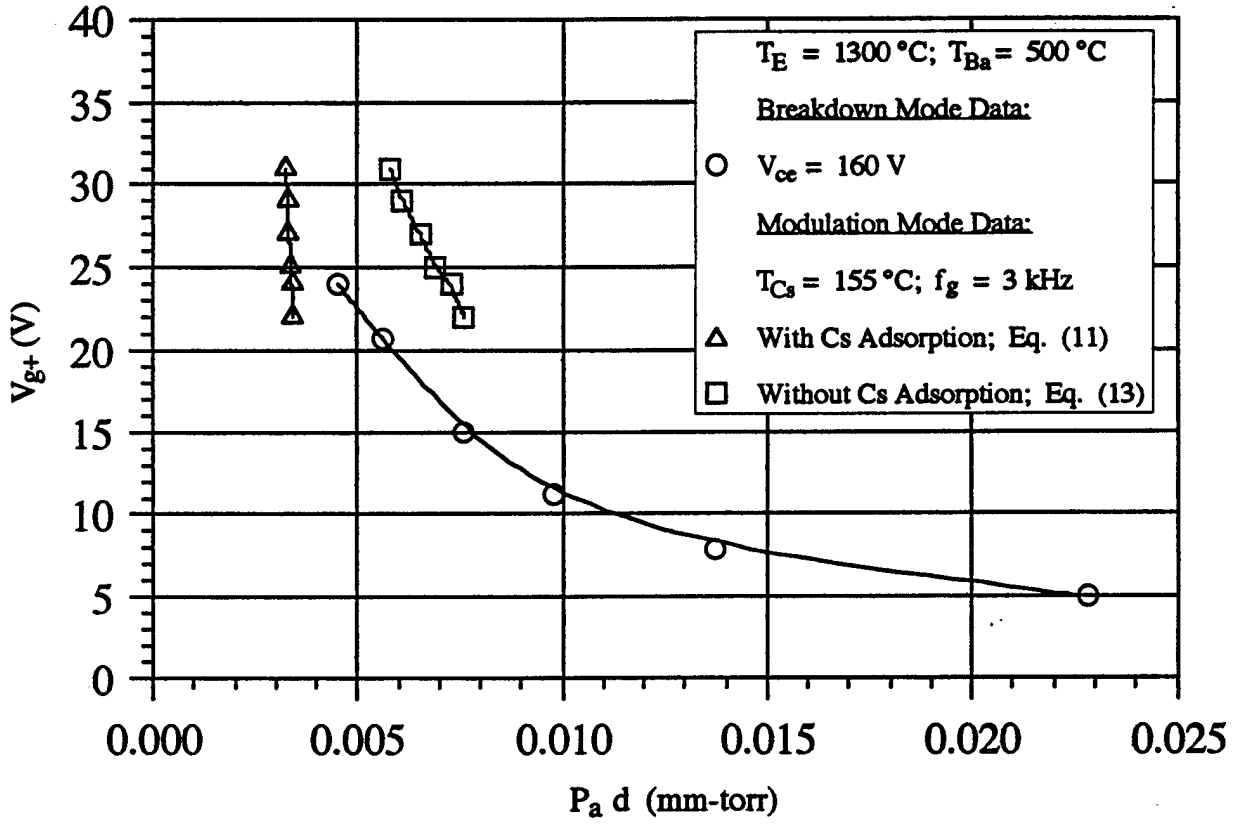

Figure 13. Effect of Cs Adsorption During Stable Current Modulation on Calculated P_ad for Ignition Compared to the Measured P_ad from Breakdown Mode Data for T_E = 1300 °C and T_{Ba} = 500 °C

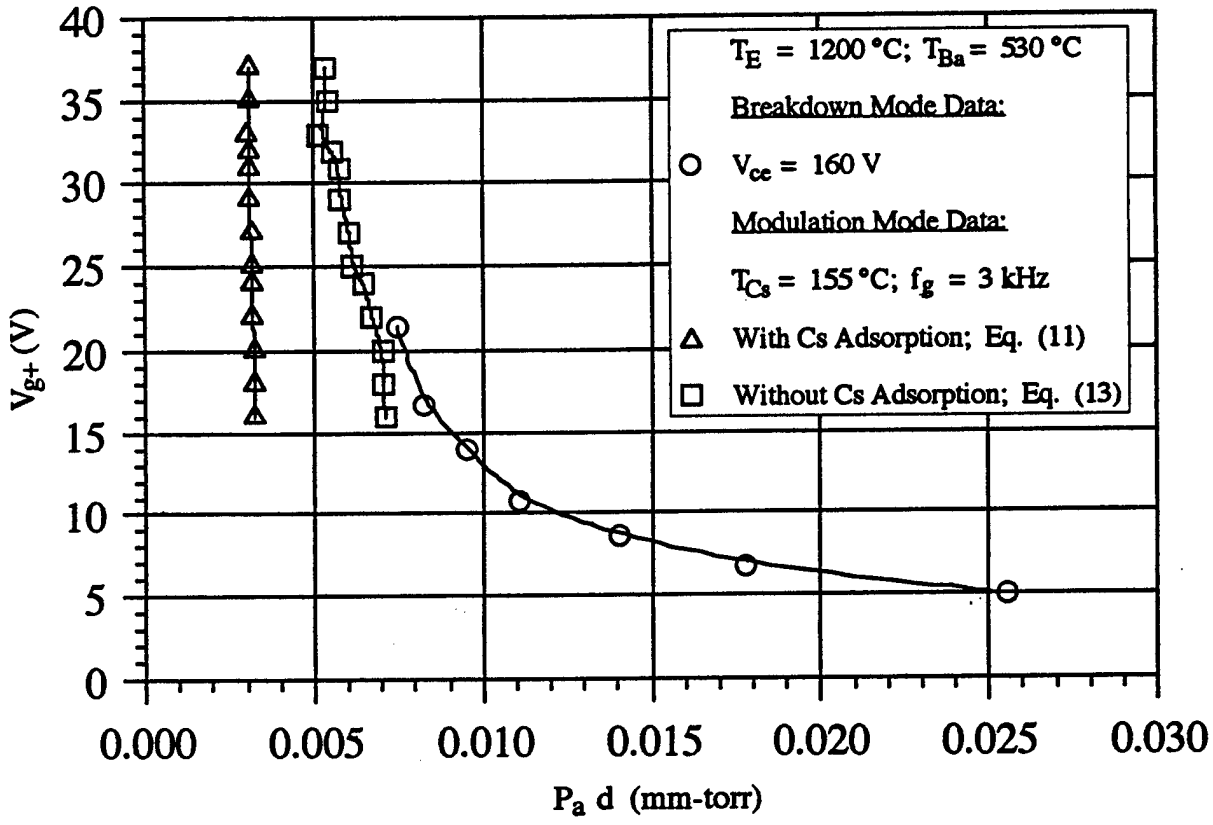

Figure 14. Effect of Cs Adsorption During Stable Current Modulation on Calculated $P_a d$ for Ignition Compared to the Measured $P_a d$ from Breakdown Mode Data for T_E = 1200 °C and T_{Ba} = 530 °C

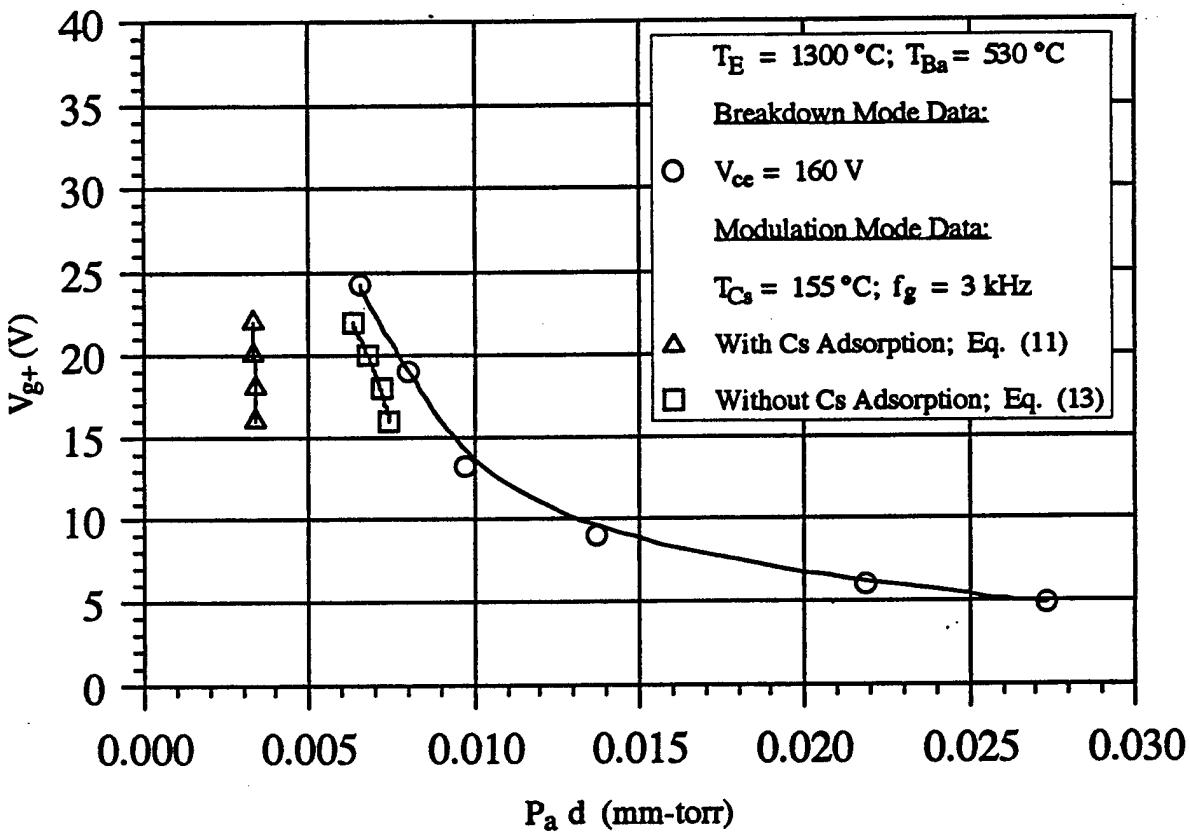

Figure 15. Effect of Cs Adsorption During Stable Current Modulation on Calculated P_ad for Ignition Compared to the Measured P_ad from Breakdown Mode Data for T_E = 1300 °C and T_{Ba} = 530 °C

to 35 V, the off-time for ignition is almost halved from 120 μs to 70 μs. Figures 16-18 show that, at a modulation time of approximately 13 ms, decreasing the grid potential for ignition from 30 V to 20 V not only increases the off-time for ignition, but also causes the current modulation of the Cs-Ba tacitron to become unstable; the application of a negative potential to the grid sometimes fails to extinguish the discharge (see Fig. 18). Consequently, the device's modulation frequency (~ 2 kHz) becomes lower than the applied modulation frequency to the grid (4 kHz). In Fig. 17, the ignition and extinguishing of the device always occurred when $V_{g+} \geq 30$ V. Because the total of V_{g+} and V_{g-} in the experiments is constant at 46 V, increasing V_{g+} automatically lowers V_{g-}. In Fig. 18 where the operating conditions are identical to Fig. 17, reducing V_{g+} from 30 V to 20 V still successfully ignites the device; however the tacitron fails to extinguish when a negative potential of 26 V is applied to the grid. The threshold value of V_{g+} for unstable modulation decreases as the Cs reservoir temperature increases, i.e. shorter off-time. For example, the V_{g+} threshold decreases from 20 V at T_{Cs} = 150 °C to about 12 V at T_{Cs} = 160 °C.

Additional results on the effects of the Cs pressure on the off-time for ignition are shown in Fig. 19. This figure compares the values of the tacitron off-time calculated from the breakdown mode and measured from the modulation mode as functions of the ignition grid potential, V_{g+}, and Cs reservoir temperature. It is interesting to note that not only does the off-time decrease when the Cs pressure is increased, as previously mentioned (Figs. 6-11), but the difference between the values of the measured and calculated off-times also decreases with increasing Cs pressure. This decrease in the difference is due to the flux from the reservoir becoming the major source of atoms going into the gap at the high Cs reservoir temperatures. This is because the density of Cs atoms in the reservoir becomes large enough to compensate for the square-root of the temperature ratios as seen in Eq. (5).

As shown in Fig. 19, for V_{g+} = 30 V, the off-time for ignition decreases from 190 μs to 110 μs as the T_{Cs} is increased from 150 °C to 160 °C, which corresponds to that previously observed in Figs. 6. Note that the lowest value of τ_{off} is only about 10 μs lower than that calculated for the breakdown mode at the same conditions.

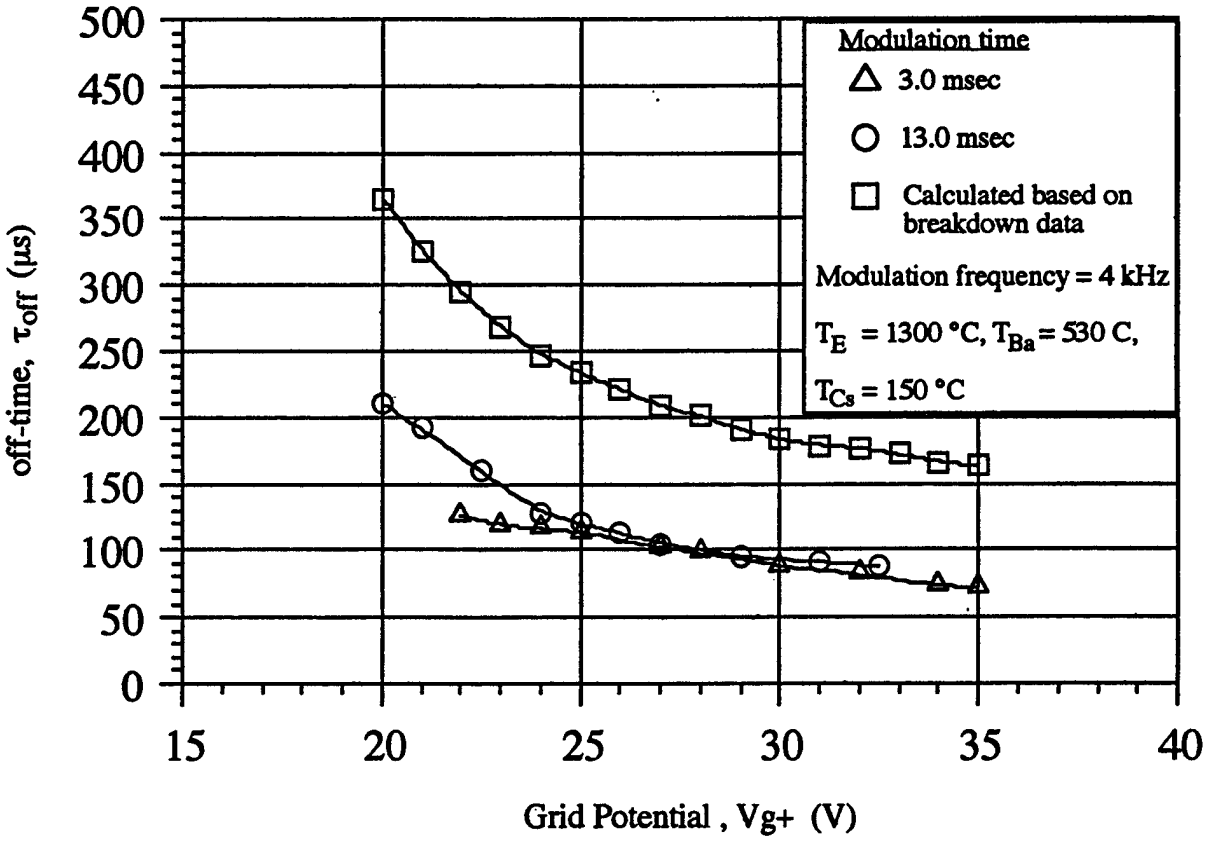

Figure 16. Comparison of the Effect of V_{g+} on the Off-time Required for Ignition in the Breakdown and Modulation Modes

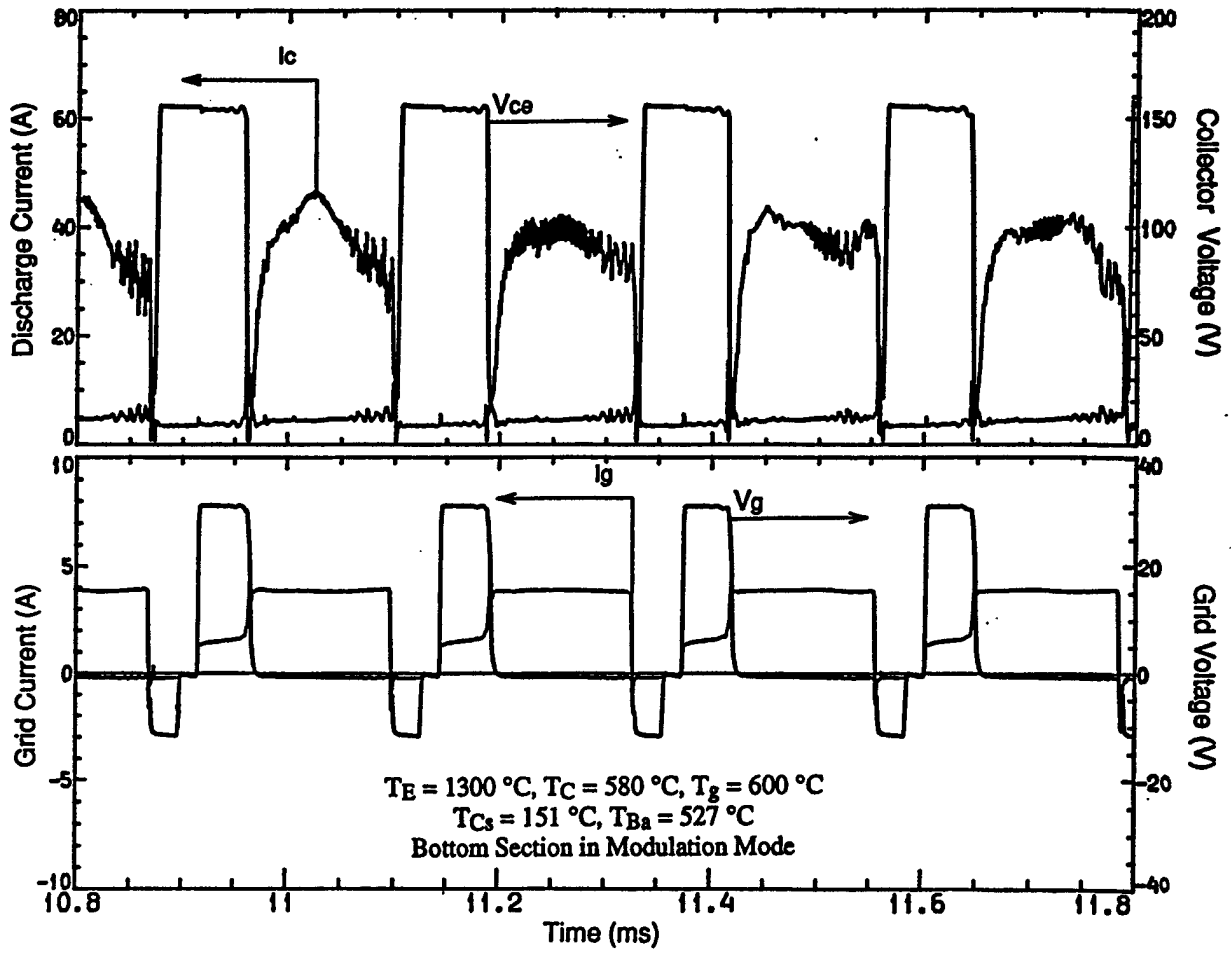

Figure 17. Typical Operation Characteristics of the Cs-Ba Tacitron for Stable Modulation at a Positive Grid Potential of 30 V and T_{Cs} = 150 °C

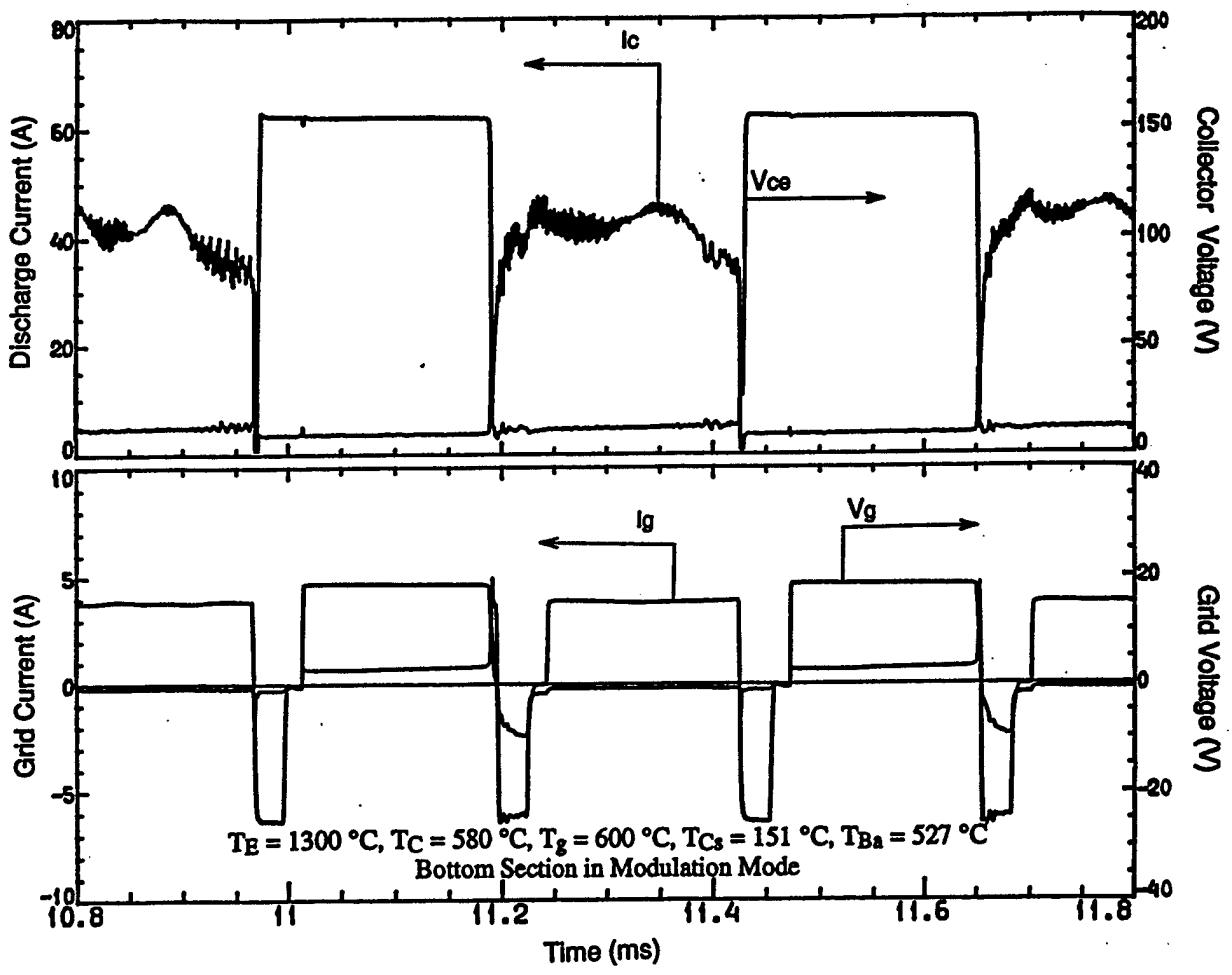

Figure 18. Typical Operation Characteristics of the Cs-Ba Tacitron for Unstable Modulation at a Positive Grid Potential of 20 V and T_{Cs} = 150 °C

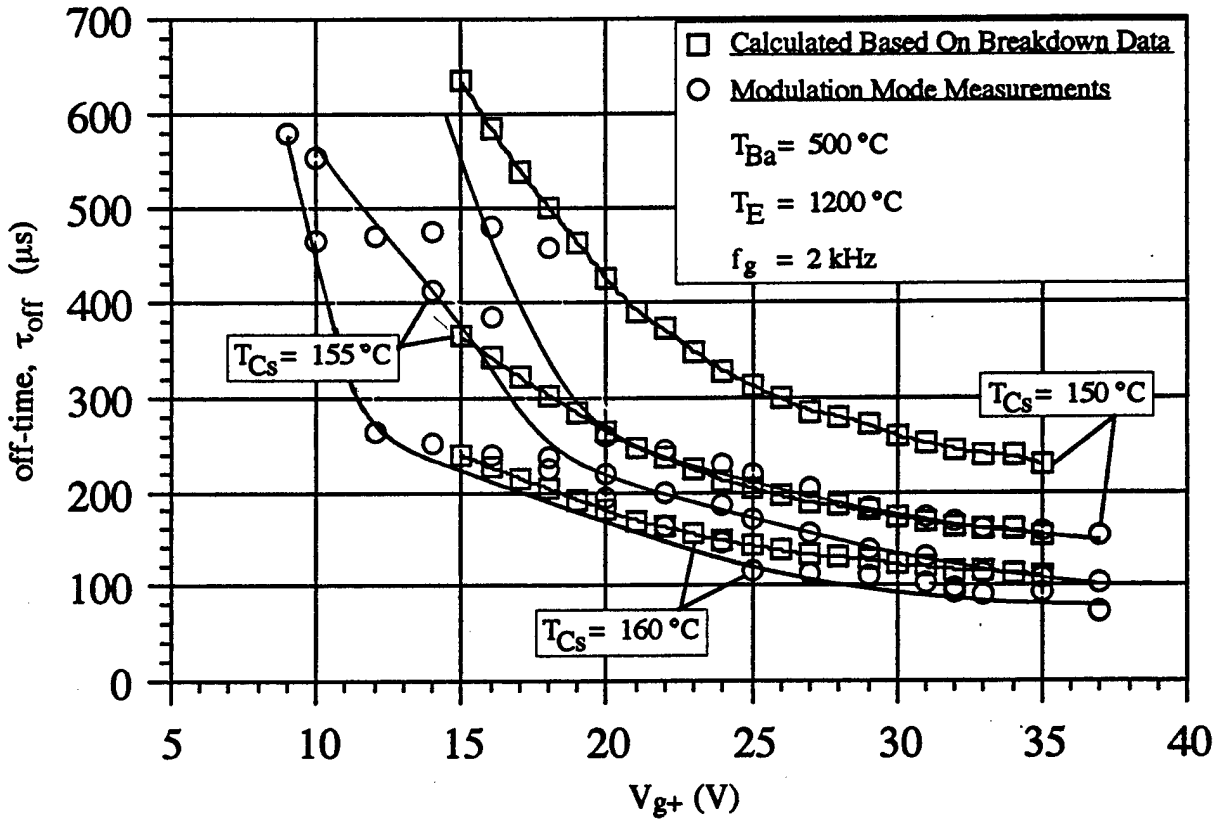

Figure 19. Effect of Cesium Reservoir Temperature on the Off-time for Ignition in the Current Modulation Mode of Operation Compared to the Calculated Value of Off-time at $f_g = 2$ kHz

The results in Fig. 20 also show, that the minimum duty cycle for stable current modulation is about 48 %. The results also show, that the duty cycle for stable current modulation increases not only with T_{Cs} but also with Vg+; but it seem to level out at about 80 %. Since P_ad is directly related to the Cs reservoir temperature, increasing the latter would reduce the off-time for ignition and increase the duty cycle of the tacitron (see Figs. 19-23). The duty cycle, η_d, is defined as *the ratio of the on-time (τ_g-τ_{off}) to the applied modulation period to the grid (τ_g).*

6.3 Ignition Conditions for Stable Current Modulation

As previously mentioned, stable modulation of the Cs-Ba tacitron occurs when ignition and extinguishing of the discharge successfully occur when a positive and a negative potential is applied to the grid, respectively. Consequently, the device modulation frequency, f_m, will be equal to the applied modulation frequency to the grid, f_g.[2] However, during stable modulation, results show that the on-time should be approximately equal to or greater than the off-time of the device, which results in a duty cycle for the tacitron in excess of 50 %. For a given f_g, the longer the off-time for ignition the shorter are the on-time and the duty cycle of the device. However, if the on-time is not long enough to lower the ion density in the gap to successfully extinguish the discharge when a negative potential is applied, the device is said to be operating in the unstable modulation mode.[2,3] As shown in Fig. 20-23, stable modulation of the tacitron occurs at a duty cycle $\geq$ 40-50 %. At a lower duty cycle, the modulation of the device becomes unstable where ignition occurs when a positive potential is applied to the grid, but the device fails to extinguish when the negative potential is applied to the grid. The results in Figs. 20-23 indicate that increasing the Cs reservoir temperature beyond 1250 °C lowers the grid potential required for ignition, but insignificantly affect the duty cycle threshold value for stable modulation. Also, increasing the emitter temperature increases V_{g+} for ignition and slightly increases the duty cycle threshold for stable modulation (~ 60 %). For $T_E \leq$ 1250 °C, the duty cycle for stable modulation is almost independent of the emitter temperature. For example, increasing the emitter temperature from 1200 °C in Fig. 20 to 1300 °C in Fig. 22 increases the duty cycle threshold from 50 % to ~ 60

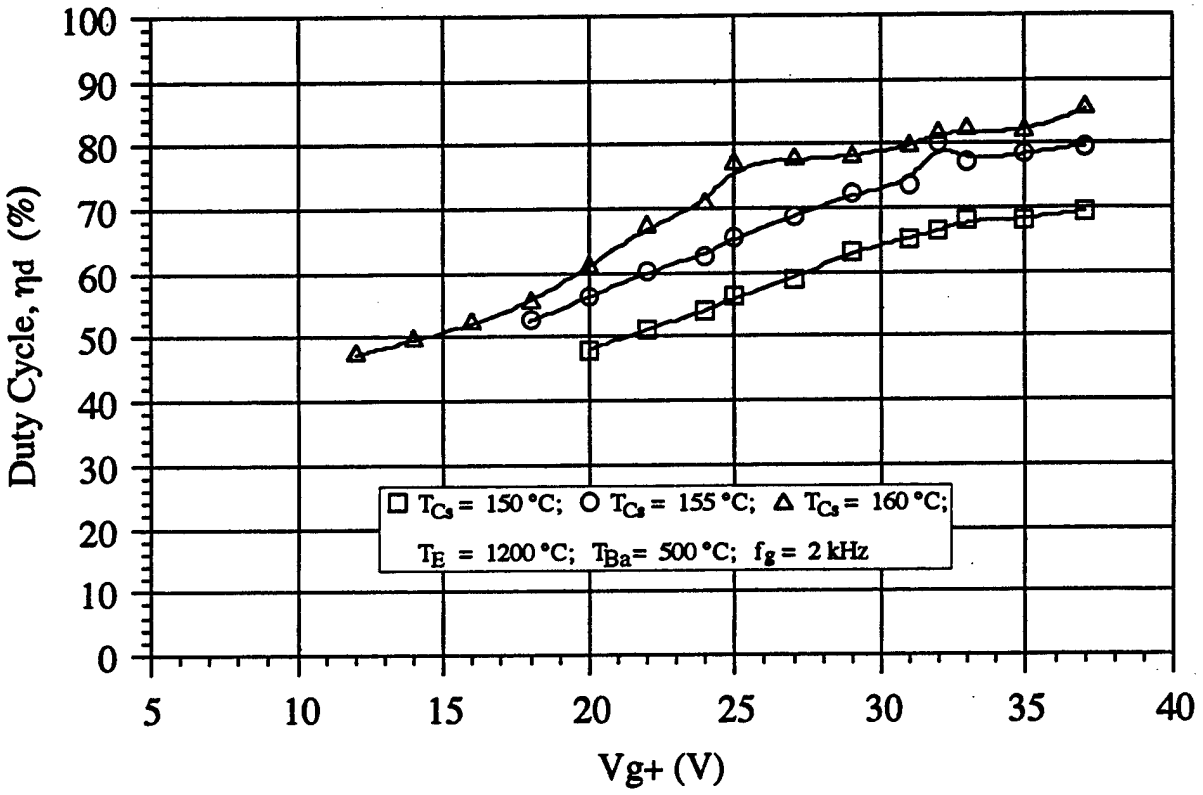

Figure 20. Effect of Ignition Grid Potential and Cesium Reservoir Temperature on the Duty Cycle of the Cs-Ba Tacitron for a f_m = 2 kHz and T_E = 1200 °C

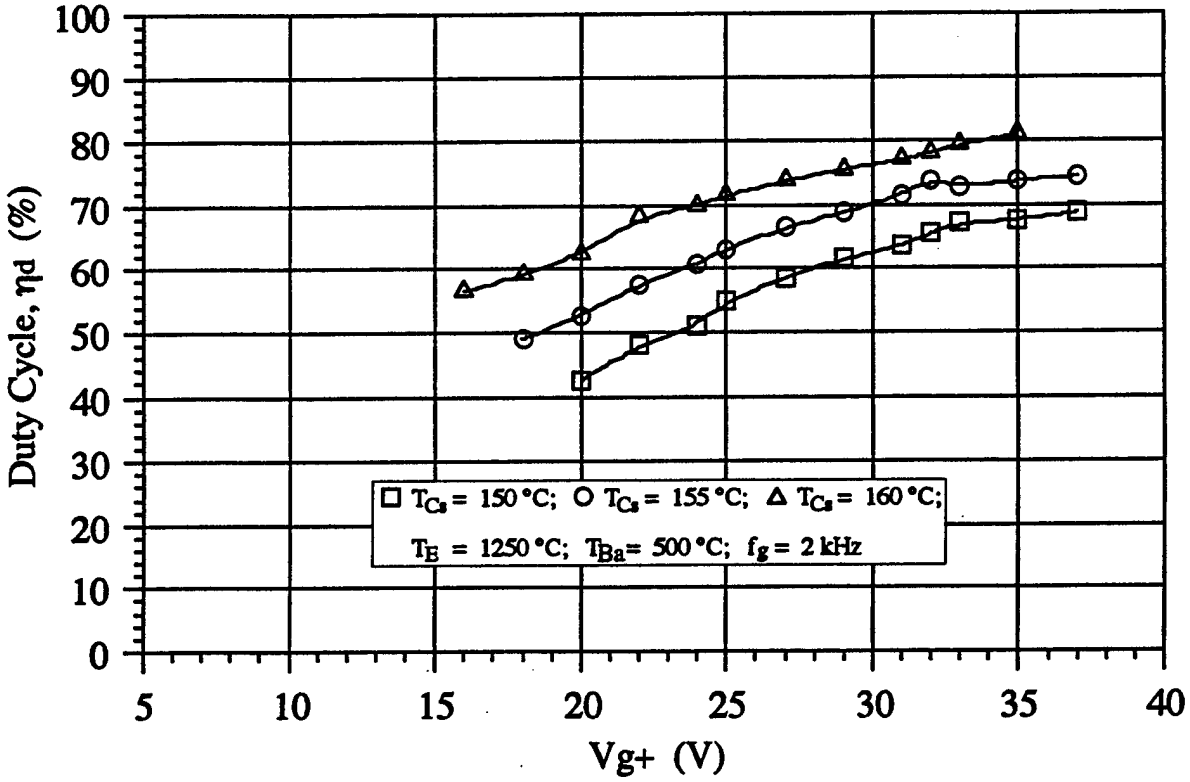

Figure 21. Effect of Ignition Grid Potential and Cesium Reservoir Temperature on the Duty Cycle of the Cs-Ba Tacitron for a f_m = 2 kHz and T_E = 1250 °C

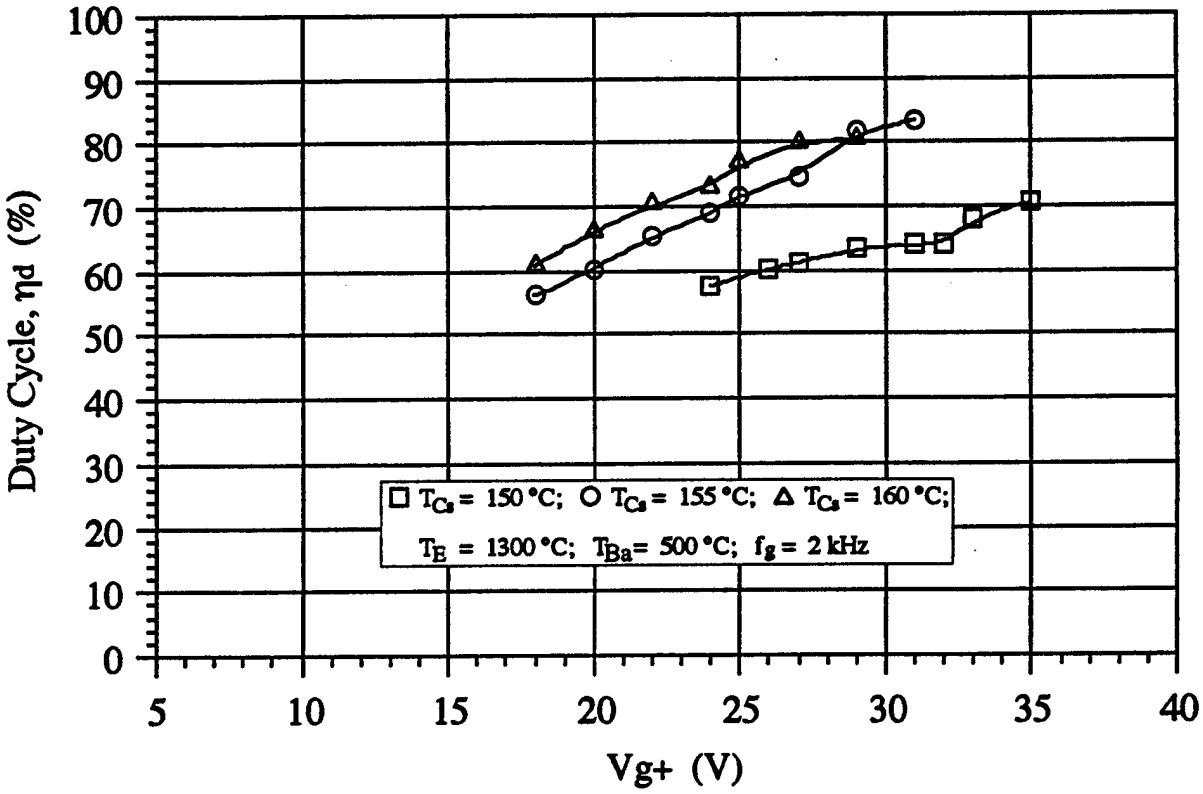

Figure 22. Effect of Ignition Grid Potential and Cesium Reservoir Temperature on the Duty Cycle of the Cs-Ba Tacitron for a f_m = 2 kHz and T_E = 1300 °C

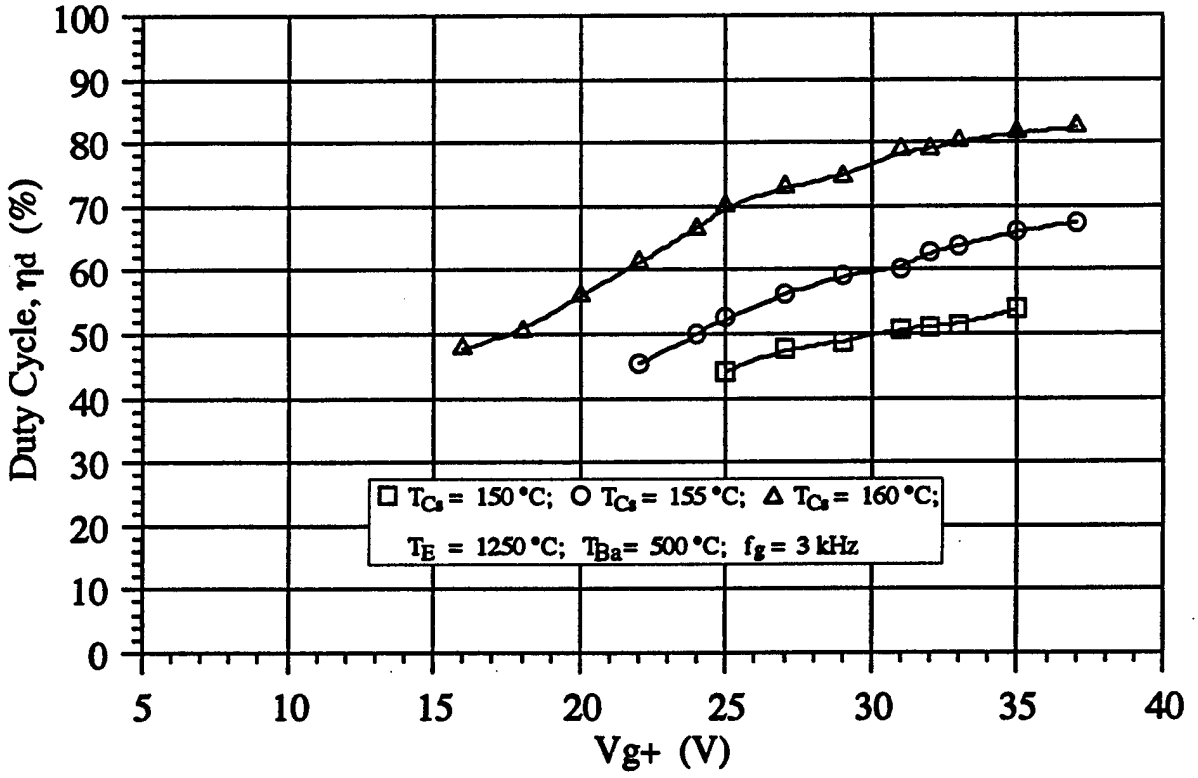

Figure 23. Effect of Ignition Grid Potential and Cesium Reservoir Temperature on the Duty Cycle of the Cs-Ba Tacitron for a f_m = 3 kHz and T_E = 1250 °C

%. As indicated earlier, increasing the Cs reservoir temperature decreases τ_{off} and hence increases the duty cycle for a given V_{g+}, or decreases V_{g+} for ignition at a given duty cycle.

Figures 20-23 also show that not only the Cs pressure but also the modulation time effects the values of V_{g+} corresponding to the duty cycle threshold for stable modulation. For example, the data delineated in Fig. 20 indicates that increasing the Cs temperature from 150 °C to 160 °C decreases V_{g+} corresponding to the duty cycle threshold for stable modulation from 20 V to as low as 12 V. Such a decrease in V_{g+} is due to the higher Cs atom flux into the gap from the reservoir. A comparison of the data in Figs. 21 and 23 at T_E = 1250 °C show that increasing the applied grid frequency from 2 kHz to 3 kHz slightly lowers the duty cycle threshold value for stable current modulation, but increases the corresponding values of V_{g+} by ~ 20 %. For example at T_{Cs} = 150 °C, when the applied grid modulation frequency is increased from 2 kHz to 3 kHz, the duty cycle threshold remains almost the same at about 48 %; however, the corresponding value of V_{g+} increases from approximately 20 V to 25 V, respectively. Such an increase in V_{g+} with f_g is due to the fact that increasing the modulation frequency proportionally decreases the off-time required for ignition and hence, lowering the Cs atom density in the gap at the time of ignition and increasing the value of V_{g+} required for ignition.

7. SUMMARY AND CONCLUSION

Experimental studies of the ignition conditions of the Cs-Ba tacitron during both breakdown and modulation modes of operation are performed. Investigated are the effects of the Cs pressure, Ba pressure, emitter temperature, collector potential and grid potential on the off-time for ignition in both modes of operation. The effect of the net Cs adsorption on the off-time during stable current modulation is found to be insignificant. Results indicate that the off-time required for ignition is strongly dependent on the Cs pressure in the gap and the ignition grid potential, but it is less dependent on the emitter temperature. At low emitter temperature ($T_E \leq$ 1250 °C), the off-time for ignition is almost independent of the Ba vapor pressure, but increass slightly with Ba vapor pressure at high emitter temperatures. Results also show that during current modulation at a

given Cs pressure, the off-time increases as the grid potential for ignition decreases. Conversely, for a given V_{g+}, the off-time required for ignition during stable current modulation decreases as the Cs pressure is increased. Increasing the modulation frequency to the grid not only reduces the value of τ_{off} for ignition but also its threshold value for stable current modulation. Experimental results demonstrate that τ_{off} should be shorter than a threshold value in order to successfully ignite the discharge for a given V_{g+}. This value is ≤ 260 μs at a grid modulation frequency of 2 kHz and is ≤ 200 μs at 3 kHz. For stable current modulation, at $V_{g+} \geq 30$ V, τ_{off} is almost independent of V_{g+}, but increases as V_{g+} is decreased and/or the emitter temperature is increased.

In the current modulation mode of operation, decreasing the positive ignition potential to the grid increases the off-time, hence decreasing the duty cycle, but could cause unstable current modulation since it simultaneously decreases the negative grid potential for extinguishing. The value of the duty cycle threshold for stable current modulation in these experiments is between 40-60 %, depending upon the grid modulation frequency and the Cs vapor pressure and to a lesser extent on the emitter temperature. It is shown that increasing the applied grid frequency negligibly affects the duty cycle threshold for stable modulation but increases the corresponding values of the ignition potential of the grid by as much as 20 %. Future research will investigate the effect of the time when the positive grid potential is applied following ignition ($\tau_{g\text{-}max}$) on the off-time for ignition and on the operation frequency attainable for stable modulation of the Cs-Ba tacitron.

ACKNOWLEDGMENTS

The authors would like to thank V. Kaibyshev, A. Borovskikh, Y. Djashiashvili and Y. Taldonov from the I.V. Kurchatov Institute for Atomic Energy, Moscow, Russia, for their help in the analysis of results and testing of the tacitron. A special thanks goes to Dr. Kaibyshev for his valuable comments and thorough review of this manuscript. Research sponsored by the Strategic Defense Initiative Organization and the Aero Propulsion and Power Directorate, Wright Laboratory, U. S. Air Force, Wright-Patterson AFB under Subcontract No. S-247-002-001, to University of New Mexico's Institute for Space Nuclear Power Studies.

REFERENCES

1 M.S. El-Genk, C.S. Murray, S. Chaudhuri, V. Kaibyshev, A. Borovskikh, Y. Djashiashvili, and Y. Taldonov, Proceedings of the 26th IECEC Conference, vol. 3, 160, Boston, MA (1991).

2 C.S. Murray, M.S. El-Genk, and V.Z. Kaibyshev, Proceedings of the 9th Symposium on Space Nuclear Power Systems, vol. 9, 417, Albuquerque, NM, (1992).

3 C.S. Murray, M.S. El-Genk, and V.Z. Kaibyshev, a companion paper submitted for consideration for publication in J. Appl. Phys. (1991).

4 V. Kaibyshev, A. Borovskikh, Y. Djashiashvili, Y. Taldonov, M.S. El-Genk, C.S. Murray and G. McDuff, Proceedings of 2nd Annual Conference of Space Power, Sukhumi, Georgia, (October, 1991).

5 G.N. Hatsopoulos, and E.P. Gyftopoulos, *Thermionic Energy Conversion*, MIT Press, Cambridge, MA, vol. 1 (1967).